THE EFFECT OF THERMALLY AND CHEMICALLY ENHANCED BIOSTIMULATION ON THE HYDRAULIC PROPERTIES OF A DISCRETE FRACTURE NETWORK IN A BEDROCK AQUIFER.

By

Reid Thomas Smith

A thesis submitted to the Department of Civil Engineering

in conformity with the requirements for

the degree of Master of Applied Science

Queen's University

Kingston, Ontario, Canada

November, 2010

Abstract

The impact of thermally and chemically enhanced biostimulation of indigenous bacteria in a fractured rock aquifer and the resulting changes in hydraulic properties of the discrete fracture network were investigated at the field scale in this study. A field trial was conducted using five 30 m deep vertical boreholes drilled into limestone and granite geological units in a 100 m^2 section of a field in Kingston, Ontario. Prior to a 14 day biostimulation experiment, pulse interference tests and tracer experiments were conducted between the various boreholes to characterize the fracture permeability and connections.

Biostimulation methods were applied using a semi-passive injection withdrawal flow field. During periods of injection withdrawal, groundwater was recirculated at 15 ±2 Lpm through an aboveground reservoir (460 L) and gravity drainage system. Recirculating groundwater temperature was raised to 20°C - 25°C and a 4.5 L sodium lactate based nutrient solution was injected once daily. During biostimulation the groundwater temperature, geochemistry, microbiology and fracture hydraulic properties between the recirculating borehole pair were monitored.

Hydraulic testing results showed that borehole transmissivity was reduced by up to 92% (injection borehole) of pre-biostimulation values and transmissivity of multiple borehole connections had been reduced by up to five orders of magnitude. The results of the tracer experiments showed an increase in solute tortuosity and arrival time and a decrease in peak concentration following biostimulation. The changes in transport observed in the tracer experiments are corroborated by heat transport measurements in the recirculation borehole pair. Microbiological and geochemical evidence of biological growth were observed in recirculating groundwater, but absent in the groundwater samples analyzed. Visual observations confirmed the

increase in biological growth, although no direct characterization of the microbial community was performed.

This study indicates the semi-passive operation of thermally and chemically enhanced biostimulation can provide a successful method for bioclogging a discrete fracture network. Pulse interference tests and tracer experiments were necessary to effectively evaluate the growth and distribution of the biobarrier, which developed beyond the influence of the injection well. Additional research is required to develop a better understanding of the factors governing biobarrier formation and longevity prior to industrial application.

Acknowledgements

Financial support for this research was provided by Queen's University, the Ontario Centres of Excellence and the Ontario Reality Corporation.

Thanks to the department staff who provided technical or administrative support for this thesis. I would specifically like to note the contributions of Maxine Wilson. Thank you to my fellow students for their advice, feedback and comedic relief throughout the course of my studies. A special thank you to Morgan Shauerte and Titia Praamsma for enduring the countless questions. The field work included in this research project would not have been possible without the assistance of Mike Gibson.

I would like to thank my supervisor, Kent Novakowski for providing me with the opportunity to conduct this research project and the advice, direction and support essential to its successful completion.

Most importantly, I would like to thank my parents and Emily for their complete support and encouragement in all my endeavours.

Table of Contents

List of Figures

List of Tables

Chapter 1.0 General Introduction

Water resources in fractured rock aquifers can play an essential role in both urban and rural water supply, agriculture, industrial use and in zones of ecological importance such as streams, wetlands and estuaries. Often, fractured rock aquifers lack significant overlying deposits of unconsolidated sediment which may act as a protective layer, resulting in water supplies that are vulnerable to contamination (Lapcevic et al, 1999). Industrial activity in areas where fractured bedrock is prevalent has produced a significant number of brownfields and contaminated sites (Steimle, 2002). Remediation efforts at these sites are frequently hampered by heterogeneous distribution of fracture networks and resulting complexity in the flow pathways. Characterization of flow and transport in fractured rock aquifers is an expensive and time consuming endeavor which further complicates the potential for the success of remediation (Berkowitz, 2002).

Sites where aqueous and/or non-aqueous phase contaminants have penetrated the fractured bedrock are increasingly common and present significant remedial problems (Steimle, 2002). Remediation of these sites has proven difficult and often impossible due to the complexity of the fracture networks as aforementioned, the quantity of contaminant captured in the rock matrix and the difficulty in delineating the source zone with existing remediation technology (Parker et al., 1994; Steimle, 2002). Although many approaches exist, the most common remedial approach at present is to control and monitor the extent of contamination by pump and treat methods. This approach requires a continuous investment over significant periods of time (Mutch et al., 1993; Steimle, 2002). Many aggressive clean up approaches involve large expenditure and massive power demand that yield mixed results (NRC, 1994).

The application of bioclogging has been proposed as a method to contain contamination in fractured rock (Ross and Bickerton, 2002). Bioclogging is usually achieved through the production of biofilms which fill or clog the groundwater flow pathways. Biofilms can develop naturally in the phreatic zone when bacterial communities adhere to a rock or porous media surface and secrete exopolymeric substances (EPS). As a remedial approach, bioclogging is induced in the subsurface by either stimulating the growth of the indigenous bacteria (biostimulation) or the addition and stimulation of foreign bacteria (bioaugmentation) (Ross and Bickerton, 2002). In both methods, the objective is to promote production of a persistent biofilm that clogs the fractures or pores to potentially reduce the effective hydraulic conductivity of the media by up to several orders of magnitude for extended periods of time (Ross, 2007), consequently providing hydraulic containment or redirection of a solute plume.

Bioclogging was originally investigated in the 1980s as a method of enhanced oil recovery by engineers in the petroleum industry (Shaw et al., 1985; Lappin-Scott et al., 1988; Cusack et al., 1990). Used to clog areas of high permeability, flooding techniques would then be employed to the low permeability zones to flush out remaining hydrocarbon reserves.

Recently, bioclogging has been increasingly explored as a remedial design for controlling both aqueous and non-aqueous contaminant transport in porous media. Some limited success has been achieved in many laboratory experiments using both fractured and porous media at varying scales (Taylor et al., 1990; Baveye et al., 1998; Sharp et al., 1999; Ross et al., 2001, Ross and Bickerton, 2002, Hill and Sleep, 2002, Castegnier et al., 2006, Charbonneau et al., 2006 and Ross et al., 2007). Very few field scale studies have been conducted, but notable success was achieved at the field scale in porous media sites with greater than 99% reduction in hydraulic conductivity observed in some cases (Jennings et al., 1995; Cunningham et al., 2003; Kim et al., 2006).

Bioclogging applications in fractured bedrock sites have received less attention to date. Only one known field study involving bioclogging in a fractured rock setting was performed by Knight (2008) and Bayona (2009) at a site in southern Ontario. Based on the results of hydraulic tests, a 65% reduction in the transmissivity of an isolated fractured interval (2.2 m packer spacing) intersecting two boreholes was observed. Significant changes to the microbiological and geochemical composition of the groundwater in the fracture were also were noted. Successful bioclogging however was limited to a single isolated fracture, and demonstrated poor persistence. Thermal stimulation was attempted, but abandoned due to ineffectiveness of the heating equipment.

The primary objective of this study is to investigate the potential for the application of biobarrier technology in discrete fracture networks. In order to examine this a field trial was conducted to investigate 1) the feasibility for the combination of chemical and thermal stimulation methods to promote significant bacterial growth in the discrete fracture network; 2) the potential for bacterial growth and biofilm development to hydraulically clog the fractures and impart changes to groundwater flow and transport pathways; and 3) the ability of hydraulic tests, tracer experiments and the measurement of groundwater geochemistry to evaluate changes in the subsurface due to bioclogging. The completion of a field trial will provide initial evidence of the potential for biobarrier technology at the scale of a discrete fracture network in a real field setting.

1.1 References

Baveye, P., P. Vandevivere, B.L. Hoyle, P.C. DeLeo and D.S. de Lozada (1998). Environmental impact and mechanisms of the biological clogging of saturated soils and aquifer materials. Critical Reviews in Environmental Science and Technology 28 (2), 123–191.

Bayona, L. (2010). Effects of in-situ stimulation of natural biofilm on groundwater flow and back diffusion in a fractured rock aquifer. Queen's University, Kingston, Ontario.

Berkowitz, B. (2002). Characterizing flow and transport in fractured geological media: a review. Advances in Water Resources, 25, 861-884.

Castegnier, F., N. Ross, R. Chapuis, L. Deschenes and R. Samson (2006). Long-term persistence of a nutrient-starved biofilm in a limestone fracture. Water Research, 40, 925-934.

Charbonneau, A., K. Novakowski and N. Ross (2006). The effect of biofilm on solute diffusion in fractured porous media. Journal of Contaminant Hydrology, 85: 212-228.

Cunningham, A. B., R. Sharp, R. Hiebert, and G. James (2003). Subsurface biofilm barriers for the containment and remediation of contaminated groundwater. Bioremediation Journal, 7, 151-164.

Cusack, F., H. Lappinscott, S. Singh, M. Derocco and J.W. Costerton (1990). Advances in microbiology to enhance oil-recovery. Applied Biochemistry and Biotechnology 24–5, 885–898.

Hill, D. and B. Sleep (2002). Effects of biofilm growth on flow and transport through a glass parallel plate fracture. Journal of Contaminant Hydrology, 56, 227-246.

Jennings, D., J. Petersen, R. Skeen, B. Hooker, B. Peyton, D. Johnstone, and D. Younge (1995). Effects of Slight Variations in Nutrient Loadings on Pore Plugging in Soil Columns. Applied Biochemistry and Biotechnology, 51/52, 727-734.

Kim, G., S. Lee, and Y. Kim (2006). Subsurface biobarrier formation by microorganism injection for contaminant plume control. Journal of Bioscience and Bioengineering, 101, 142-148.

Knight, L. (2008). The effect of biostimulation on geochemical and microbiological conditions in an isolated dolostone fracture. Queen's University, Kingston, Ontario.

Lapcevic, P.A., K.S. Novakowski, E.A. Sudicky (1999). Groundwater Flow and Solute Transport in Fractured Media. Chapter 17, The Handbook of Groundwater Engineering. CRC Press LLC.

Lappin-Scott, H.M., F. Cusack, and J.W. Costerton (1988). Nutrient resuscitation and growth of starved cells in sandstone cores: A novel approach to enhance oil recovery. Applied and Environmental Microbiology, 54, 1373-1382.

Mutch, R.D., J.I. Scott, and D.J. Wilson, (1993). Clean-up of fractured rock aquifers: Implications of matrix diffusion. Environmental Monitoring and Assessment, 24, 45-70.

NRC (1994). Alternatives for groundwater cleanup. National Academy Press, Washington, D.C., USA.

Parker, B.L., R.W. Gillham and J.A. Cherry (1994). Diffusive disappearance of immiscible-phase organic liquids in fractured geologic media. Ground Water, 32(5): 805-819.

Prescott, L.M., J.P. Harley, and D.A. Klein (2002). Microbiology, 5th Ed. McGraw-Hill, New York.

Ross, N., R. Villemur, L. Deschênes, and R. Samson (2001). Clogging of a limestone fracture by stimulating groundwater microbes. Water Research, 35, 2029-2037.

Ross, N. and G. Bickerton (2002). Application of biobarriers for groundwater containment at fractured bedrock sites. Remediation, Summer 2002, 5-21.

Ross, N., K. S. Novakowski, S. Lesage, L. Deschenes, and R. Samson (2007). Development and resistance of a biofilm in a planar fracture during biostimulation, starvation, and varying flow conditions. Journal of Environmental Engineering Science, 6, 377-388.

Sharp, R.R., A.B. Cunningham, J. Komlos, and J. Billmayer (1999). Observation of thick biofilm accumulation and structure in porous media and corresponding hydrodynamics and mass transfer effects. Water Science and Technology, 39(7):(1999)195-201.

Shaw, J.C., B. Bramhill, N.C. Wardlaw, and J.W. Costerton, (1985). Bacterial fouling in a model core system. Applied Environmental Microbiology, 49(3), 693-701.

Steimle, R. (2002). The state of the practice: characterizing and remediating contaminated groundwater at fractured rock sites. Remediation, Summer 2002, 23-33.

Taylor, S.W., P.C.D. Milly, and P.R. Jaffe (1990). Biofilm growth and the related changes in the physical properties of a porous media 2. Permeability. Water Resources Research 26 (9), 2161–2169.

Chapter 2.0 Field investigation of thermally and chemically enhanced biostimulation of indigenous bacteria and the development of a biobarrier in a discrete fracture network

2.1 Introduction

Remediation of contaminated fractured media can prove to be a complex and expensive endeavor (Steimle, 2002) due to the complexity of flow pathways in a discrete fracture network (Berkowitz, 2002), potential for contaminants to diffuse into the rock matrix and the difficulty in delineating the source zone with existing remediation technology (Mutch et al., 1993; Parker et al., 1994). Bioclogging (or biobarrier construction) has been proposed as a hydraulic containment method of contaminated groundwater (Ross and Bickerton, 2002; Cunningham et al., 2003). Bioclogging provides an attractive alternative to existing containment technologies because it requires relatively little financial investment, doesn't involve excavation (useful for sites where access to the subsurface may be limited) and is believed to involve minimal maintenance over long time periods (Hiebert et al., 2001; Cunningham et al., 2003).

Biobarrier construction is achieved by the stimulation of microbial activity leading to increased biological growth that causes clogging in the discrete fractures and the permeable voids of geological units (Ross and Bickerton, 2002). Although significant increases in biomass alone can reduce transmissivity, it is the production of extracellular polymeric substances (EPS) that supports biofilm development and the potential for significant bioclogging (Allison, 2003). The EPS are made up of polysaccharides, proteins, nucleic acids and lipids. They form a structural

matrix for microbial cells, govern adhesion to surfaces and function in a wide variety of biofilm processes (Flemming et al., 2010).

Bioclogging experiments have been studied since the 1980s for application as a method of enhanced oil recovery (Shaw et al., 1985; Lappin-Scott et al., 1988; Cusack et al., 1992; Davey et al., 1998). Recent studies focusing more on the remedial applications have been undertaken with some success (at least 99% reduction in hydraulic conductivity or transmissivity) at both the bench and field scale in porous media settings (Vandevivere and Baveye, 1992; Cunningham et al., 2003; Kim, 2004), and in single fracture experiments at the bench scale (Hill and Sleep, 2002; Arnon et al., 2005). The only known existing bioclogging study in a fractured rock field setting was completed by Knight (2008) and Bayona (2009) on an isolated dolostone fracture at a southern Ontario field site. Bioclogging was achieved in the fracture and reductions in transmissivity reached 65% relative to pre-biostimulation values. Building on the successful components of this previous work, the objective of this field trial was to investigate the feasibility of applying this technology to a discrete fracture network at the field scale.

2.2 Site Description

The field site is located in an industrial area of north Kingston, Ontario (Figure 1). The bedrock geology consists of Precambrian metamorphic and plutonic rocks with highly variable lithologies typical of the Canadian Shield (Ontario Geological Survey, 2009). The Precambrian is located at approximately 26 m below ground surface (bgs) on site. Several Paleozoic units of the Gull River formation overlie the Precambrian bedrock. These include: interbedded silty dolostone,

lithographic to fine crystalline limestone, shale and fine grained calcareous quartz limestone (Armstrong and Carter, 2006). Unconsolidated overburden is approximately 4 m deep in the boreholes used for the experiment. The overburden consists of fine grained silt to silty clays common among Lansdowne series soils (SLEC, 2002).

Five HQ (96 mm diameter) boreholes were drilled and cored vertically in May 2008 to characterize the study area. Well locations, elevations, depth are outlined in Table 1 and illustrated in Figure 1 and Figure 2.

Figure 1. Overview map of site location in Kingston, Ontario. The location of project boreholes are represented by the blue star and presented in Figure 2.

Figure 2. Expanded view of project boreholes region from Figure 1.

Table 1. Location and depth of project boreholes.

Borehole	Northing	Easting	Elevation (masl)	Total Depth (BTOC)
MTK200	4902218.064	378988.461	88.569	31.34
MTK201	4902207.869	378988.232	88.637	28.14
MTK202	4902217.407	378978.215	88.349	31.31
MTK203	4902212.888	378983.188	88.54	31.31
MTK204	4902207.346	378977.973	88.526	32.19

masl: meters above sea level
BTOC: below top of casing

The fracture network pervading the site was investigated initially in June 2008 using the constant head injection test (CHIT) method (Novakowski et al., 2000). Three major sub-horizontal fracture zones with measured transmissivities greater than 10^{-7} m^2/s were identified (Schauerte, 2011) (Figure 2) at approximately 12 mbgs (FZ1), 25 mbgs (FZ2) and 31 mbgs (FZ3).

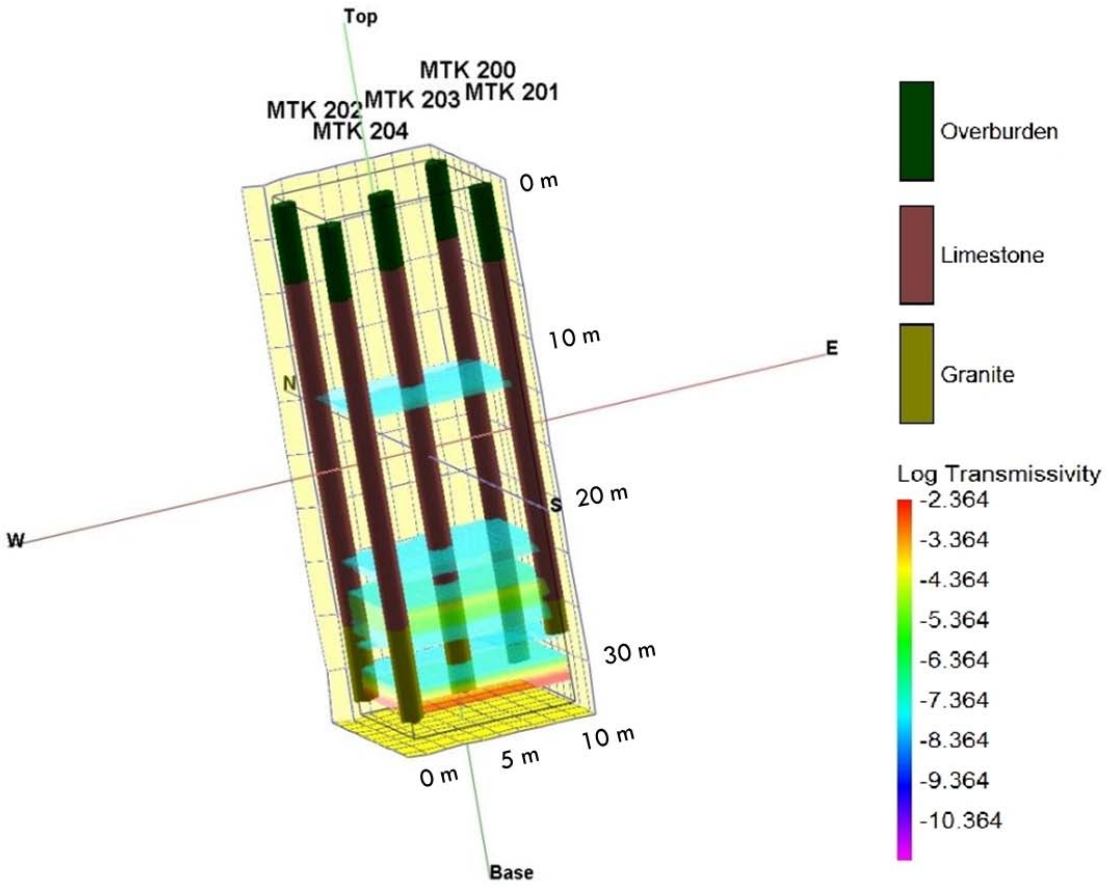

Figure 3. Fracture zone transmissivity (10^{-8} m^2/s or greater) and lithology of project boreholes. Approximate depth of each geological unit is: overburden, 0 – 4 mbgs; limestone, 4 - 26 mbgs; and granite 26 – 32 mbgs.

In the summer of 2009, open borehole pulse interference tests were conducted to examine the hydraulic properties of the fracture connections within the borehole network (Appendix G).

An injection withdrawal recirculation system was selected for nutrient delivery during biobarrier construction. Using the pulse interference test and CHIT data, a series of injection-withdrawal

tracer experiments were performed in the fall of 2009 to explore borehole pair options for groundwater recirculation. The experiments were performed under open borehole conditions, between boreholes MTK201, MTK202, MTK203 and MTK204 with varying injection withdrawal orientations and flow rates. Boreholes MTK202 and MTK203 were determined to be a viable well pair for recirculation of the proposed nutrient mixture and biobarrier formation. For complete results of the tracer experiments see Appendix A.

Previous site assessment work by M.S Thompson & Associates (1998, 1999), Dillon Consulting Limited (2001) and SNC Lavelin Engineers and Constructors (2002) have included investigation of groundwater flow direction on site. Shallow bedrock and overburden groundwater flow was determined to occur in a North to Northeast direction, although some mounding occurs to the immediate east side of the site. The mounding may result in a local northeast to southwest flow direction across the designed project area. The determined direction of groundwater flow for the shallow groundwater systems could not be applied to the deeper groundwater flow system in the underlying Precambrian rocks, which didn't exhibit a distinct direction of flow at the scale of the five project boreholes.

2.3 Characterization Methodology

2.3.1 Introduction

Site characterization methods discussed in the following sections were performed prior to, during and following biostimulation to evaluate biobarrier performance. The biostimulation phase began on February 5, 2010 (Day 1) and continued through February 18, 2010 (Day 14) and the

starvation phase is termed for the time period from February 19, 2010 (Day 15) to April 2, 2010 (Day 57). Project dates during the field trial will be referred to as the number of days following the commencement of biostimulation.

2.3.2 Hydraulic Tests

Falling head slug tests were performed on each borehole to investigate the bulk transmissivity of the project boreholes prior to biostimulation and throughout the field trial. All tests were performed under open borehole conditions. Pre-trial testing included three separate slug testing events on: August 18, 2009, November 1, 2009 and January 30, 2010. Results from these tests were used to investigate response linearity for each borehole, generate an averaged pre-trial value for borehole transmissivity and investigate repeatability and precision for the test. Testing also occurred during biostimulation on Days 5, 9, 11, 12, 14 and in the starvation phase on Days 18, 29 and 57.

For all falling head slug tests the slug was created by the pseudo-instantaneous (10 to 15 seconds) addition of 10.0 L (± 0.5 L) of water and changes in water level were measured with Solinst™ Leveloggers Model 3001 M5. Measurements were recorded at intervals of 0.5 and 1.0 seconds at an accuracy of 0.003 m. The control borehole was selected as MTK200, as it is hydraulically isolated from the induced flow field and thermal and chemical stimulation. Analysis was conducted using the High K Hvorslev model described in Butler and Garnett (2000). The type curves used were generated using equations described in Zlotnik and McGuire (1998).

Pulse interference tests (PITs) were performed as an extension of slug testing to monitor changes in transmissivity of the hydraulic connections within the borehole network. PITs were also used to investigate values of bulk storativity for the experimental area. Pulse interference testing was completed for open borehole connections during all slug testing events. The control borehole pair was selected as MTK200 and MTK201 as this connection would be hydraulically isolated from the induced flow field and thermal and chemical stimulation. In addition, isolated interval PITs where intervals in both the source and observation boreholes were isolated using packers were completed pre-trial (January 15, 2010) and following the biostimulation phase on Day 30.

The borehole interval testing targeted the FZ2 and FZ3 fracture zones (Figure 2). Each fracture zone was isolated using pneumatic packers, connected to the surface with 2 inch and 1 3/8 inch internal diameter polyvinyl chloride (PVC) standpipe at the source and observational wells respectively. In all tests Solinst^{TM} Levelogger Model 3001 M5 were used to measure changes in water level. Measurements were recorded at intervals of 0.5 and 1.0 seconds with an accuracy of 0.003 m.

Analysis of the both open borehole and isolated interval PITs were performed using the graphical method presented in Novakowski (1989). Graphical method results were confirmed using manual type curve fitting generated from Equation 17 presented in Novakowski (1989).

The distance between source and observation wells was calculated using northing and easting UTM coordinates from a GPS satellite survey, assuming predominant fracture planes were orientated approximately parallel with surface topography which exhibits minimal relief over the project area. An averaged value for bulk storativity was generated using pre-trial results from

testing between all borehole pairs. This value was kept constant for calculations throughout the field trial.

2.3.3 Tracer Experiments

The injection-withdrawal experiments were conducted under open borehole conditions between the recirculation boreholes MTK 202 (injection) and MTK 203 (withdrawal) to investigate changes in solute transport properties. The tracer experiments were conducted once pre-trial (January 26, 2010) and once following the biostimulation phase on Day 35.

The tracer experiments were completed by establishing a steady state flow system between the injection and withdrawal boreholes with recirculation through a heated aboveground reservoir and injection system (Figure 3). Steady flow was assumed once values of hydraulic head in both wells showed no significant variation (± 40 mm). Injection and withdrawal flow rates were established at 15.0 ± 2.0 Lpm using a Grundfos Redi-Flo2 submersible pump for withdrawal and gravity drainage for injection. The natural water level in the injection and withdrawal boreholes was located at equivalent elevations (approximately 80 masl) prior to both tracer experiments.

Once steady state conditions were met, approximately 10 g (pre-trial: 10.38 g and post-trial: 10.59 g) of the fluorescent dye tracer Lissamine FF (coefficient of free-water diffusion; 4.5×10^{-10} m^2/s) were instantaneously introduced into the heated aboveground reservoir as a powder and mixed into solution using a 12 volt shaft trolling motor. The volume of the heated aboveground reservoir was approximately 360 L and the total volume of the entire recirculation network excluding the

fracture planes, was 610 L for both tracer experiments. For a more complete description of the dimensions of the recirculation system components refer to Appendix B.

The recirculated groundwater was heated to 20°C to 25°C for the duration of both the pre-trial and post-trial tracer experiments and the Lissamine tracer was detected using a Turner Designs model 10-AU field fluorometer and flow through cell that discharged into the aboveground reservoir (Figure 3). The water level in each borehole was measured using Solinst™ Levelogger Model 3001 M5 and hydraulic head data was recorded using a CR10X Campbell Scientific Data Logger. The fluorometer was calibrated prior to each tracer experiment. Calibration curves and regression analysis results are presented in Appendix C.

2.3.4 Groundwater chemistry and microbiology

Bulk groundwater samples were collected and analyzed for general chemistry, microbiology and redox processes parameters. Sampling events were conducted pre-trial (October 26, 2009 and November 2, 2009), during biostimulation (Day 4, Day 9) and once post-stimulation (Day 19). Groundwater samples were collected after purging at least one well volume at less than 5.0 ±0.5 Lpm from the withdrawal well (MTK203) and analyzed at Caduceon Environmental Laboratories in Kingston, Ontario. Groundwater samples were collected directly from a Grundfos Redi-Flo2 submersible pump and connecting hose then containerized, preserved and analyzed in accordance with Canadian Association for Laboratory Accreditation (CALA) accredited methods.

Water chemistry of recirculating groundwater was measured using a handheld YSI 556 multi-probe unit and recorded 2 to 4 times a day.

2.4 Biobarrier Construction

2.4.1 Introduction

The biostimulation field trial focused on biobarrier development in the discrete fracture network in the project boreholes. Thermal and chemical methods of biostimulation are employed to provide the substrate and environmental conditions necessary to increase microbial activity. A semi-passive recirculating borehole pair was used to distribute the nutrients and heat to the subsurface, and provide access to groundwater for visual and analytical monitoring. The combination of forced and natural gradient conditions were used to maximize mixing and spatial influence of biostimulation.

2.4.2 Experimental apparatus

Based on pre-trial site characterization, borehole MTK202 was selected as the injection borehole and MTK203 was selected as the withdrawal well for thermal and chemical stimulation. A semi-passive, injection withdrawal recirculation system was selected for nutrient delivery where a recirculation flow field was operated for 8 h to 10 h each day then terminated allowing the subsurface to return to natural groundwater flow conditions. This system was selected to maximize dispersive mixing between the nutrient solution and ambient groundwater (Devlin and

Barker, 1996). A Grundfos Redi-Flo2 submersible pump was used for extracting water from the open withdrawal borehole at a constant rate of 15.0 ± 2.0 Lpm. The groundwater was pumped to an insulated aboveground reservoir (460 L galvanized steel tank), which provided a point of access for thermal and chemical application, tracer injection and monitoring of various parameters throughout the field trial. The reservoir was gravity drained into 35 m of 25.4 mm internal diameter (ID) polyethylene tubing coiled in an insulated box (910 mm× 910 mm× 910 mm) adjacent the reservoir. The heated aboveground reservoir, polyethylene tubing and insulated casing and two working surfaces were all housed within a 3.7 m×6.1 m×2.4 m enclosed tent. From the polyethylene tubing the water drained through 16.5 m of 13 mm internal diameter hose to MTK202. In order to facilitate the high rate of gravity driven flow, the injection point was selected at 6.20 m below the top of the MTK 202 well casing. Adjustments of injection point depth to maintain an equivalent flow rate were made throughout the field trial as biological growth and thermal deformation of the tubing, decreased the internal volume of the injection system and consequently reduced volumetric flow rates. Boreholes MTK 200, MTK 201 and MTK 204 were left open for hydraulic testing and as points of observation for the duration of the project. A schematic diagram of the aboveground recirculation system is illustrated in Figure 3, and complete dimensions of the system are provided in Appendix B.

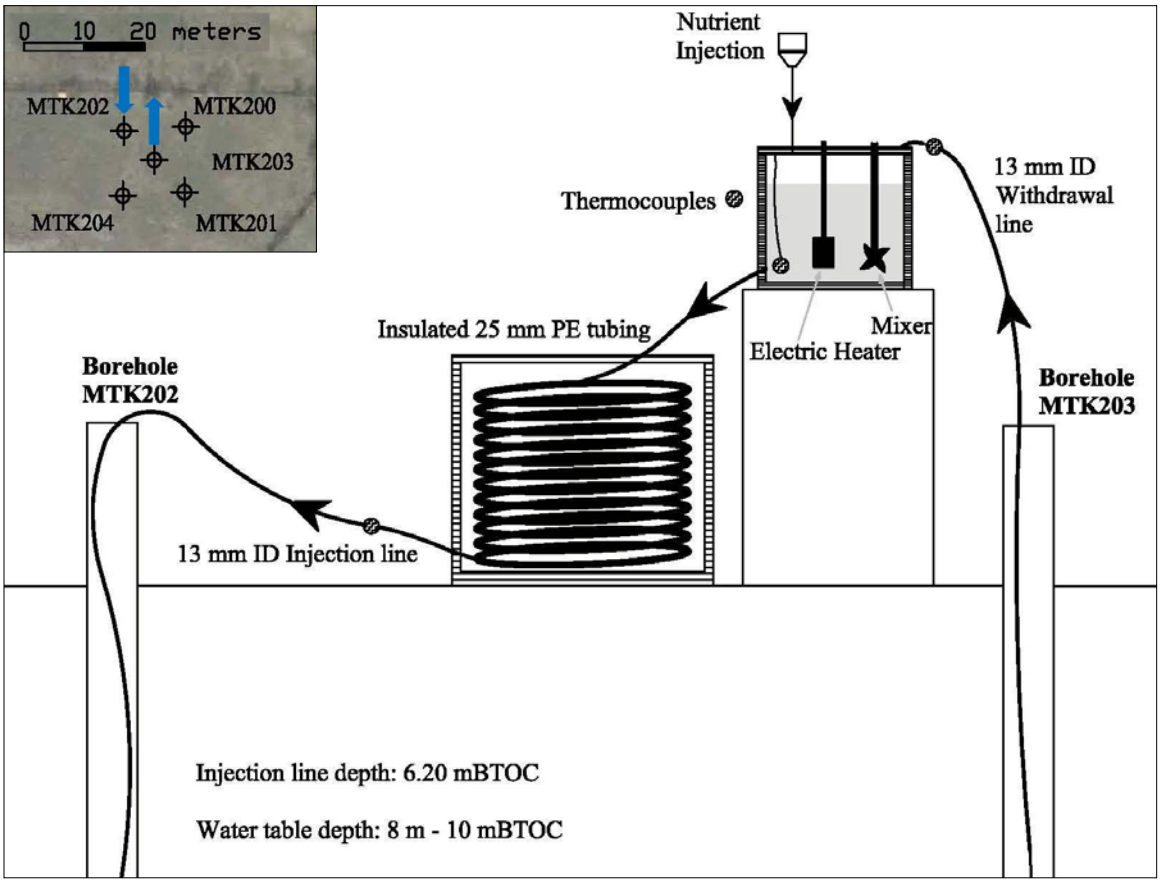

Figure 4. Schematic diagram of aboveground recirculation system.

2.4.3 Chemical Stimulation

Chemical stimulation was provided by the daily addition of a nutrient solution to the recirculating groundwater in the aboveground heated reservoir. Nutrient addition took place only after a steady flow field had been achieved. The nutrient package was added instantaneously and mixed into solution using a 12 volt shaft trolling motor as with the tracer experiments. Recirculation of groundwater between the injection and withdrawal boreholes was completed for 6 hours to 9 hours each day following nutrient injection. The standard molar ratio of carbon to nitrogen to phosphorus (C:N:P) for microbial growth is 100:10:1 (Bouchez et al., 1995; Leys et al., 2005).

This biostimulation field trial used a nutrient solution in a 100:11:2 (C:N:P) molar ratio comprised of 60% w/w Sodium Lactate and commercially available liquid fertilizers. Variation from the standard molar ratio (100:11:2) was done to maximize available quantities of the nutrient sources. See Appendix D for calculations and Appendix E for a record of all nutrient additions.

2.4.4 Thermal Stimulation

Heat was added to the recirculation system using a Chromalox TLC-210A-048/240V immersion heater powered by a Wacker G25 Mobile Generator. The immersion heater was mounted to a stand directly over the reservoir aligning the two 34 inch copper heating elements down the centerline, approximately 10 cm above the bottom. Heater output was controlled by a Chromalox AR-115-KIT-4 thermostat kit and groundwater temperature at the reservoir outlet was maintained at 20°C to 25°C for the duration of groundwater recirculation each day. Type T (copper-constantan) thermocouples were used to monitor the changes in groundwater temperature in the aboveground component of the recirculation system. Thermocouples were mounted to monitor recirculating groundwater at the discharge to the reservoir from MTK203, the outlet of the reservoir, and the end of the 25.4 mm ID polyethylene coil prior to injection into MTK202 (Figure 4). Thermocouple readings were recorded on the CR10X Datalogger. Temperature measurements in the injection and withdrawal boreholes were recorded at 5 minute and 10 minute intervals using Solinst Leveloggers Model 3001 M5 with an accuracy of 0.05°C and range of -10°C to 40°C. The leveloggers were located at approximately 10 m and 20 m BTOC in each borehole.

2.5 Results

2.5.1 Hydraulic Testing

During the biostimulation phase (Day 1 to Day 14) testing was limited to the injection and withdrawal boreholes. Slug testing events performed post-biostimulation included all project boreholes.

Decreases in transmissivity from pre-trial values were observed in MTK201, MTK202, MTK203 and MTK204. The greatest decrease in transmissivity was seen in the injection well; MTK202, with a maximum of a 92 % reduction of pre-trial transmissivity values (Figure 5). This reduction was observed at Day 14, the final day of the biostimulation phase. Reduction in borehole transmissivities reached 64 %, 72 % and 63 % for boreholes MTK201, MTK203 and MTK204 respectively (Figure 4 and 5). These reductions were all observed at either Day 18 or Day 22 slug testing events for these boreholes.

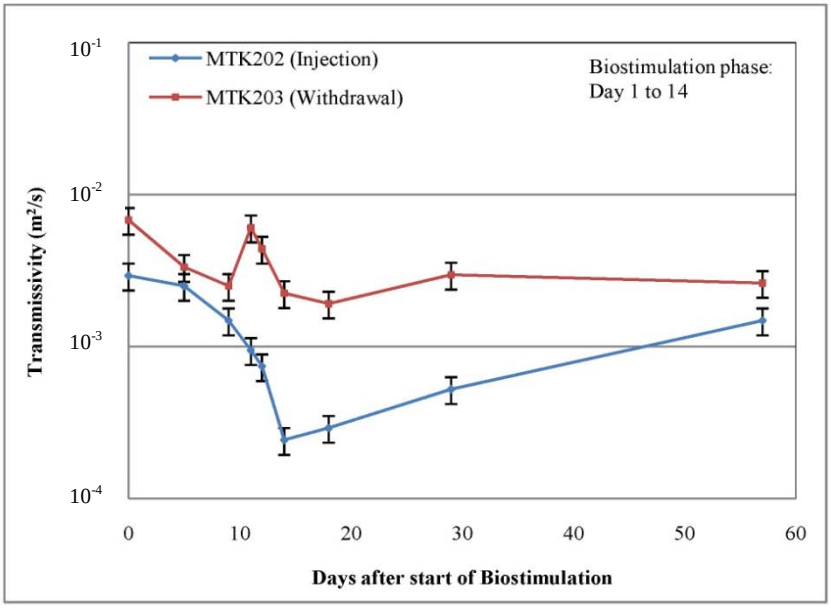

Figure 5. Changes in borehole transmissivity in the injection (MTK202) and withdrawal boreholes (MTK203) during the biostimulation field trial. Lines connecting data points are interpretive should only be used as a guide.

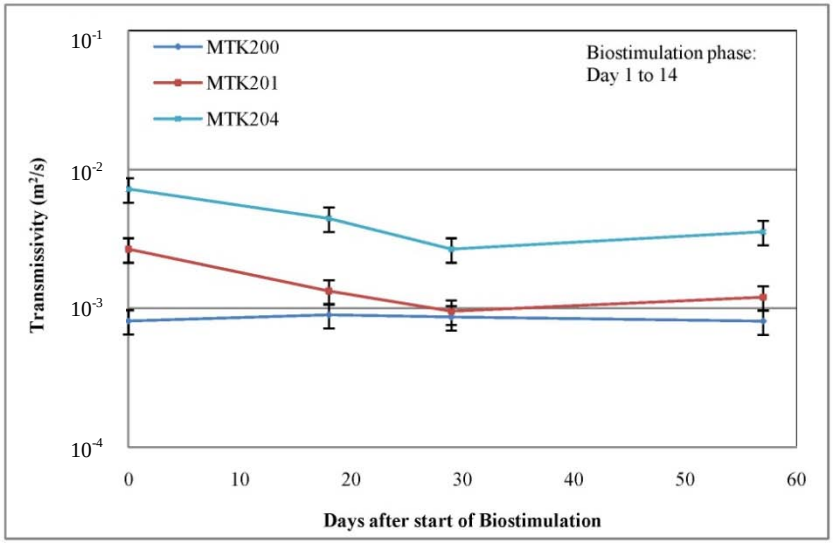

Figure 6. Changes in borehole transmissivity at boreholes MTK200, MTK201 and MTK204 during the biostimulation field trial. Lines connecting data points are interpretive should only be used as a guide.

Oscillatory, underdamped responses described in Van Der Kamp (1976) were observed in pre-trial testing of boreholes MTK202, MTK203 and MTK204 (Appendix F). These boreholes also yielded the three largest estimates of borehole transmissivity. During the biostimulation phase, as borehole transmissivity was reduced, the responses in MTK202 and MTK203 transitioned to critically damped, then overdamped. Responses to slug tests in MTK204 remained consistently underdamped to critically damped throughout the field trial. Response data obtained from MTK200 and MTK201 remained overdamped and critically damped respectively, throughout the field trial.

Hydraulic testing results from the control borehole and pre-biostimulation testing were used to assess the range of error in transmissivity values calculated. Relative standard deviations were determined for each control data set (Table 2) and the largest value (20%; MTK203, Pre-Trial)

was used as a conservative range of error (error bars on Figure 4 and Figure 5) for slug testing completed throughout the field trial.

Table 2. Slug testing results for the control borehole (MTK200) and pre-biostimulation testing at MTK202 and MTK203.

Borehole Transmissivity (m^2/s)							
Borehole	**n**	**Maximum**	**Minimum**	**Range**	**Mean**	**Standard Deviation**	**Relative Standard Deviation**
MTK200 (Control)	5	9.3×10^{-4}	7.0×10^{-4}	2.3×10^{-4}	8.4×10^{-4}	6.9×10^{-5}	8%
MTK202 (Pre-Trial)	3	3.4×10^{-3}	2.5×10^{-3}	8.8×10^{-4}	2.9×10^{-3}	2.9×10^{-4}	10%
MTK203 (Pre-Trial)	3	8.9×10^{-3}	4.9×10^{-3}	4.0×10^{-3}	6.8×10^{-3}	1.4×10^{-3}	20%

Pre-trial slug testing results showed good agreement with existing constant head injection testing results. The pre-trial slug test results also exhibited response linearity with respect to slug volume suggesting the effect of non-linear mechanisms were not significant and supporting the High K Hvorslev model for analysis. The transmissivity results calculated for all slug tests performed throughout the field trial are presented in Appendix F.

Pre-trial pulse interference testing between all borehole pairs yielded a mean storativity of 4.5×10^{-5} with an average standard deviation of 6.6×10^{-5}. A review of literature indicated this value to be higher than typically observed (Lapcevic, et al., 1999, Milloy, 2007 and Gleeson, 2009) and the storativity was set at 1×10^{-5} for all open borehole calculations (b = 20 m) and

1×10^{-6} for all isolated fracture interval calculations (b = 2.1 m to 2.6 m). The storativity value was fixed in order to provide a stable comparison of transmissivity throughout the field trial.

For testing under open borehole conditions, the largest reductions in transmissivity were observed in the hydraulic connection between boreholes MTK202, MTK203 and MTK204 all of which experienced reductions of up to five orders of magnitude from pre-trial values (Figure 6 and Table 3).

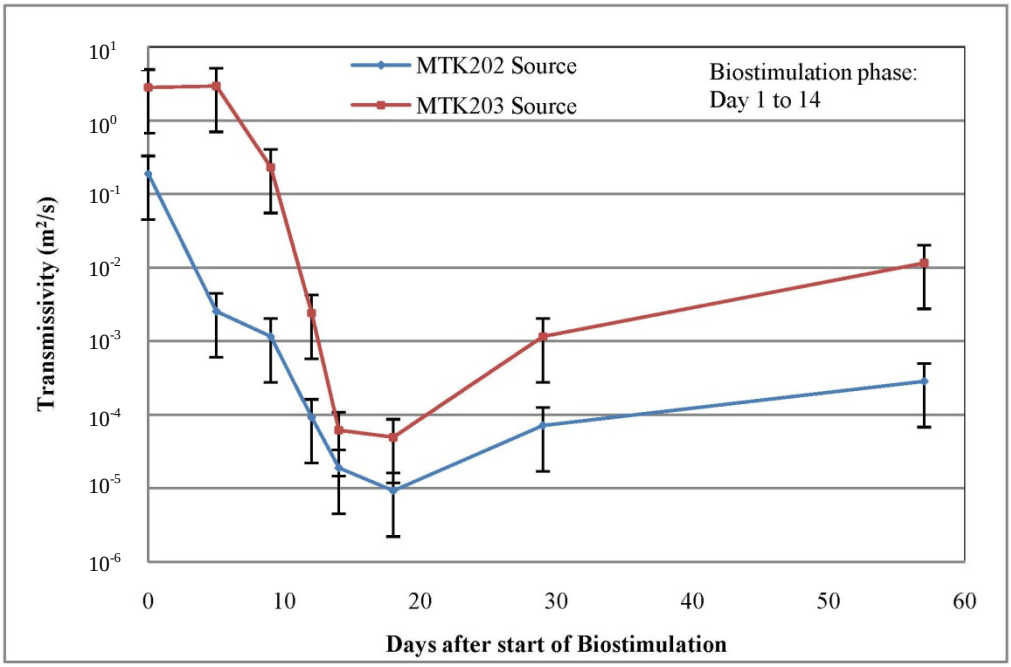

Figure 7. Changes in transmissivity of the injection (MTK202) and withdrawal (MTK203) borehole connection during the biostimulation field trial. Lines connecting data points are interpretive should only be used as a guide.

Table 3. Transmissivity (m^2/s) results of the borehole fracture connections prior to and following biostimulation.

Source Borehole	Observation Borehole	Pre-Biostimulation Average	Day 18	Day 29	Day 57	T_{min}/T_i
MTK200	**MTK201**	9.2×10^{-4}	1.4×10^{-3}	2.3×10^{-3}	8.2×10^{-4}	8.9×10^{-1}
	MTK202	2.8×10^{-4}	3.4×10^{-5}	5.1×10^{-5}	3.1×10^{-4}	1.2×10^{-1}
	MTK203	5.1×10^{-4}	2.0×10^{-3}	6.3×10^{-4}	4.2×10^{-4}	8.3×10^{-1}
	MTK204	8.1×10^{-4}	7.7×10^{-4}	6.6×10^{-4}	5.1×10^{-4}	6.3×10^{-1}
MTK201	**MTK200**	5.8×10^{-2}	2.9×10^{-1}	3.5×10^{-1}	7.3×10^{-2}	1.3×10^{0}
	MTK202	5.4×10^{-3}	1.2×10^{-4}	3.6×10^{-4}	1.0×10^{-3}	2.2×10^{-2}
	MTK203	6.9×10^{-1}	5.1×10^{0}	3.8×10^{0}	3.5×10^{0}	5.1×10^{0}
	MTK204	9.2×10^{-2}	9.2×10^{-3}	6.6×10^{-3}	3.1×10^{-2}	7.1×10^{-2}
MTK202	**MTK200**	1.5×10^{-3}	1.9×10^{-5}	3.3×10^{-5}	2.0×10^{-4}	1.3×10^{-2}
	MTK201	1.7×10^{-3}	2.8×10^{-5}	4.6×10^{-5}	4.3×10^{-4}	1.6×10^{-2}
	MTK203	1.9×10^{-1}	9.2×10^{-6}	7.1×10^{-5}	2.8×10^{-4}	4.9×10^{-5}
	MTK204	1.5×10^{-1}	1.2×10^{-4}	9.9×10^{-5}	7.7×10^{-4}	6.7×10^{-4}
MTK203	**MTK200**	9.7×10^{-3}	2.1×10^{-3}	3.7×10^{-2}	6.6×10^{-2}	2.2×10^{-1}
	MTK201	2.3×10^{-1}	5.1×10^{0}	2.3×10^{-1}	5.8×10^{0}	1.0×10^{0}
	MTK202	2.8×10^{0}	4.9×10^{-5}	1.2×10^{-3}	1.2×10^{-2}	1.8×10^{-5}
	MTK204	1.4×10^{0}	5.8×10^{-3}	5.3×10^{-2}	1.2×10^{-1}	4.2×10^{-3}
MTK204	**MTK200**	5.2×10^{-3}	1.2×10^{-3}	$1.5\times10\text{-}^{3}$	3.1×10^{-3}	2.4×10^{-1}
	MTK201	6.6×10^{-2}	4.2×10^{-3}	2.9×10^{-3}	6.6×10^{-3}	4.4×10^{-2}
	MTK202	2.9×10^{0}	2.4×10^{-4}	7.7×10^{-4}	3.1×10^{-2}	8.4×10^{-5}
	MTK203	1.4×10^{-1}	3.3×10^{-1}	6.1×10^{-3}	1.0×10^{-2}	4.3×10^{-4}

T_i: Pre-Biostimulation average transmissivity (m^2/s)

T_{min}: Lowest measured transmissivity (m^2/s) value following the commencement of biostimulation

During the biostimulation phase (Day 1 to Day 14) testing was limited to the injection and withdrawal boreholes. Changes in test response data during the biostimulation phase was initially observed on the first round (Day 5) of testing and reductions in transmissivity continued until a maximum measured reduction of over five orders of magnitude was attained on Day 18. A rebound in transmissivity values between the boreholes MTK202 and MTK203 was first observed on Day 29, over two weeks after the termination of biostimulation on Day 14.

Borehole MTK204, located downstream from MTK202 and MTK203, experienced a maximum decrease in connection transmissivity of five and four orders of magnitude with boreholes MTK202 and MTK203, respectively. The maximum decrease in connection transmissivity was observed immediately post biostimulation, on Day 18 (with MTK202) and Day 29 (with MTK203).

The transmissivity results from PITs between the control borehole pair and pre-biostimulation results between the injection/withdrawal borehole pair were used to assess the accuracy of transmissivity values. Relative standard deviation was calculated for each control data set and the largest value (76%; MTK203 to MTK202, Pre-Trial) was used as a conservative range of error (error bars on Figure 6) for the pulse interference testing.

Table 4. Pulse interference testing results for the control borehole pair (MTK200, MTK201) and pre-biostimulation testing at MTK202 and MTK203.

Borehole Transmissivity (m^2/s)							
Borehole Pair	**n**	**Maximum**	**Minimum**	**Range**	**Mean**	**Standard Deviation**	**Relative Standard Deviation**
MTK200 to MTK201 (Control)	4	2.3×10^{-3}	8.2×10^{-4}	1.5×10^{-3}	1.4×10^{-3}	0.00050	36%
MTK201 to MTK200 (Control)	4	3.5×10^{-1}	5.8×10^{-2}	3.0×10^{-1}	1.9×10^{-1}	0.13	66%
MTK203 to MTK202 (Pre-Trial)	3	4.0×10^{-1}	3.5×10^{-2}	3.7×10^{-1}	1.9×10^{-1}	0.14	76%
MTK202 to MTK203 (Pre-Trial)	3	5.4×10^{0}	7.5×10^{-1}	4.6×10^{0}	2.8×10^{0}	1.7	61%

Pre-biostimulation pulse inference testing of isolated FZ2 and FZ3 fracture connections (Figure 2) yielded transmissivities of 1.4×10^{-6} m^2/s and 2.5×10^{-5} m^2/s respectively. Vertical connectivity was observed between the fractured zones. Following biostimulation transmissivity of the FZ3 connection was reduced by two orders of magnitude and no change was observed in the FZ2 connection.

Complete results of pulse interference testing on isolated fractured intervals in MTK202 and MTK203 are found in Appendix G.

2.5.2 Tracer Experiments

The tracer breakthrough curve (BTC) measured during the pre-stimulation January 26, 2010 tracer experiment reached a maximum peak 17% of the calculated injection concentration at 64

min after injection (Figure 7). The tracer BTC measured during the post-stimulation March 11, 2010 dipole tracer experiment reached a maximum peak 11% of the calculated injection concentration at 67 min after injection (Figure 7). All data beyond the final measured sample (start of the solid line) was extrapolated using power law trendlines that were generated using the measured decay data. Equations and their regression analysis with the measured data can be found in Appendix A.

The recirculation of the tracer prevented the estimation of mass recovery investigation as inflection points for the re-arrival at the withdrawal borehole were not easily identified. As a result of the recirculation, simulation of the tracer experiments using either an analytical or numerical model is not tractable (Gelhar et al., 1996), and was not undertaken.

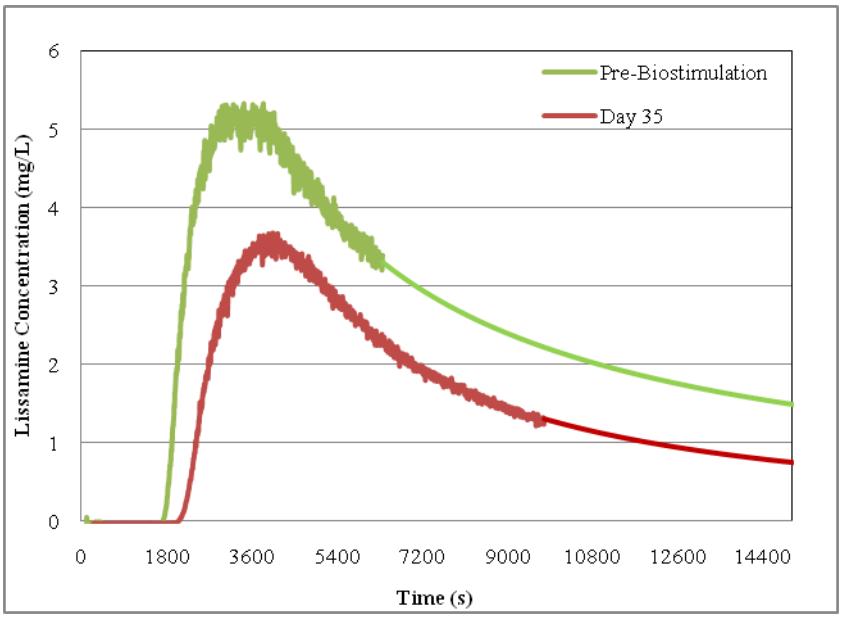

Figure 8. Lissamine concentration breakthrough curves measured from dipole tracer experiments performed pre-biostimulation and post-biostimulation (Day 35). The smooth section of each curve represents extrapolated values.

2.5.3 Thermal Stimulation

Thermal measurements in the injection and withdrawal boreholes were recorded during the field trial. These measurements are presented in Figure 8 and Figure 9. Maximum daily temperature rise in the injection borehole averaged 8.2°C and 7.9°C at 10 m and 20 m BTOC respectively. In the withdrawal borehole, maximum daily increase in temperature averaged 0.25°C and 0.37°C at 10 m and 20 m BTOC respectively. Baseline groundwater temperature was estimated to be 9.6°C at all monitored locations. This was determined using pre-trial temperature readings at 10 m BTOC over three days with a Solinst™ Levelogger Model 3001 M5. Maximum daily temperature rise for each day was estimated manually using the temperature measurements shown in Figure 8

and Figure 9. Temperature spikes are due to temporary changes in the experiment apparatus, primarily for maintenance of the recirculation system. These temperature readings were not included in averaging the daily maximum temperature data set.

Thermocouple readings collected at the aboveground reservoir and injection line during the field trial were used to maintain an injection temperature of 20-25°C into borehole MTK202. This was achieved with the exception of February 18, 2010, when the injection temperature was maintained at 35-40°C.

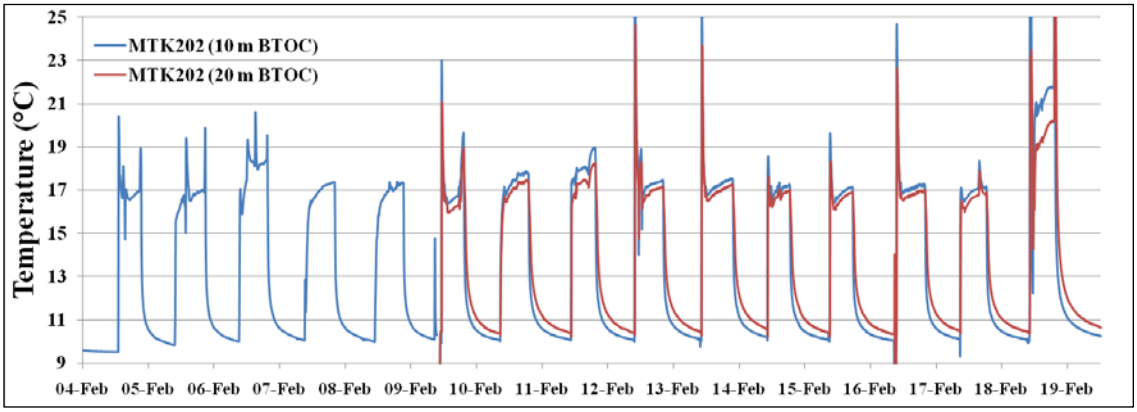

Figure 9. Temperature measurements in borehole MTK202 at 10 m and 20 m BTOC during the biostimulation field trial.

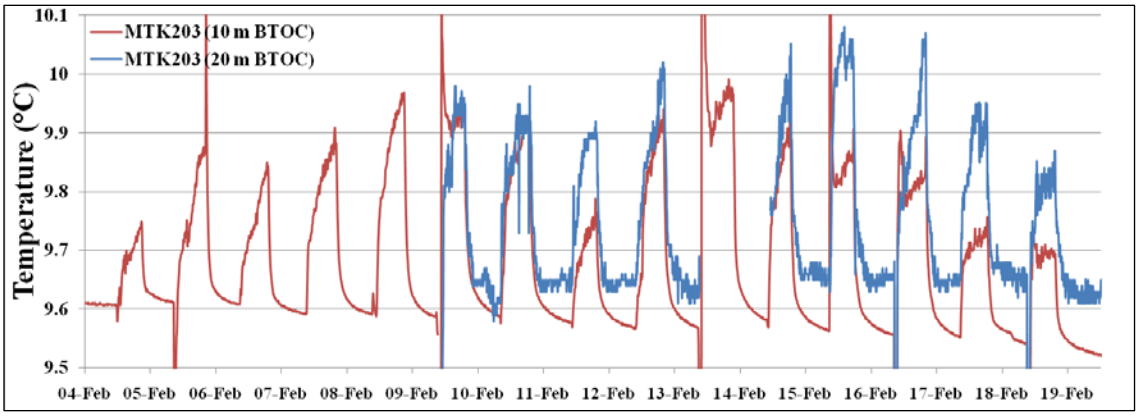

Figure 10. Temperature measurements in borehole MTK203 at 10 m and 20 m BTOC during the biostimulation field trial.

The thermocouple readings of the withdrawn groundwater (Figure 4) were not a valid indicator of groundwater temperature at the pump, located at 23 m depth in MTK203. Heat loss during transport in the tubing through the water column and outside air, and then warming of the tubing in the enclosed tent prevented an accurate measurement of groundwater temperature at this location.

2.5.4 Groundwater Chemistry and Microbiology

Groundwater chemical and microbiological analysis was performed by Caduceon Environmental Laboratories on bulk groundwater samples collected pre-trial on February 8 (Day 4) February 13 (Day 9) and February 23 (Day19). Complete results are provided in Appendix H. Analytical results for microbiological parameters, redox processes and general chemistry parameters were reported. No identifiable trends were observed.

Daily monitoring of recirculating groundwater was conducted using a handheld YSI 556 multi-probe unit. Noticeable decreases during the biostimulation phase were observed for dissolved oxygen, pH and oxidation reduction potential (ORP). This is illustrated in Figure 10 and Figure 11. Complete results of daily YSI measurements are presented in Appendix I.

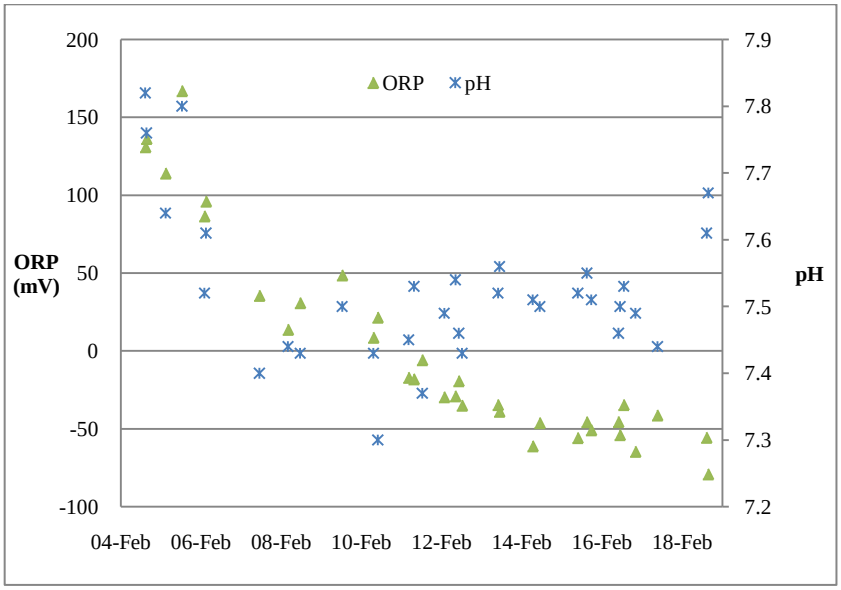

Figure 11. Oxidation reduction potential (ORP) and pH measurements from the recirculating groundwater throughout biostimulation.

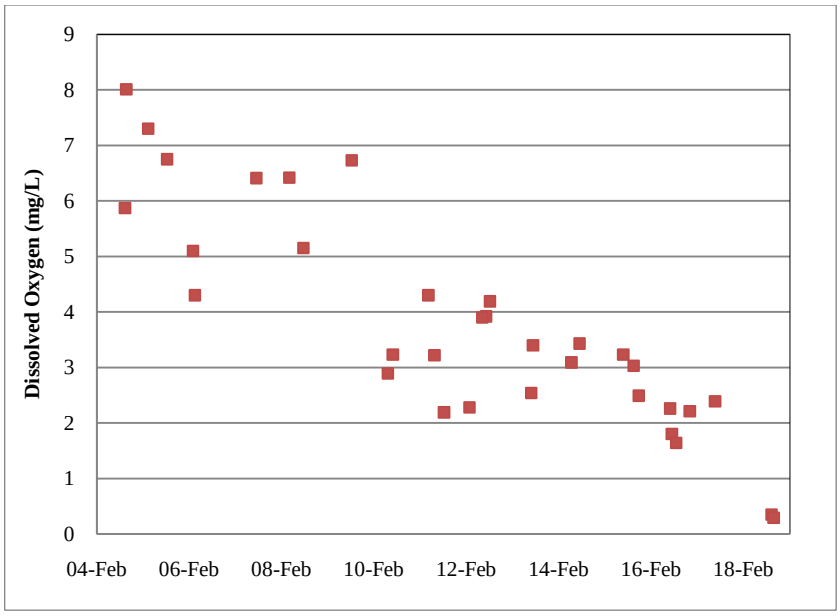

Figure 12. Dissolved oxygen measurements from the recirculating groundwater throughout biostimulation.

2.6 Discussion of Results

2.6.1 Hydraulic testing

Prior to biobarrier development three major sub-horizontal fracture zones (Figure 2) with measured transmissivities greater than 10^{-7} m^2/s were identified using constant head injection testing (Schauerte, 2011). Results of pulse interference tests (Table 3) determined the fracture connections between boreholes MTK202, MTK203 and MTK204 to be the most transmissive ($>10^{-1}$ m^2/s). Hydraulic connections from borehole MTK201 to all other project boreholes were identified (10^{-3} m^2/s to 10^{0} m^2/s), although the shallower depth of this borehole prevented intersection with the most transmissive fracture zone (FZ3). Borehole MTK200 exhibited the

least transmissive fracture connections to all other project boreholes ($<10^{-3}$ m^2/s) and was located up gradient from the injection borehole during recirculation and natural groundwater flow conditions. Transmissivity values of the borehole connections determined from pulse interference testing were up to three orders of magnitude larger than transmissivities estimated by CHITs and slug tests. This may suggest the presence of linear interwell features where the predominance of flow occurs in direct streamlines between the boreholes (Novakowski, 1988). The completion of several tracer experiments identified groundwater solute transport connections from borehole MTK203 to MTK201 and MTK 204 under natural hydraulic gradient conditions (Appendix A).

Following biostimulation, measured changes in slug test results detected bioclogging within the range of influence of all project boreholes, with the exception of the control borehole (MTK200). This confirms the poor groundwater transport connection from the injection borehole to the control under forced and natural hydraulic gradient conditions. The most extensive bioclogging occurred in the injection borehole (MTK202), withdrawal borehole (MTK203) and borehole MTK204 which is the second most transmissive fracture connection to the injection borehole (Figures 6 and Table 3). MTK204 is also located downstream of the recirculation borehole pair under a natural hydraulic gradient suggesting the drift of nutrients and/or heat.

Pulse interference testing post-biostimulation identified bioclogging in the fracture connections between the injection and withdrawal boreholes, as well as in the fracture connections from boreholes MTK204 and MTK201 to each other and the recirculating borehole pair. Maximum reductions in transmissivity were equivalent to, or exceeded results found in many bench scale studies (Hill and Sleep, 2002; Arnon et al., 2005; Castegnier et al., 2006; Ross et al., 2007). The limitation of significant biological growth to the site of nutrient injection has been a common problem in bioclogging studies. The increased spatial distribution of growth observed in this field trial may have been a result of the high pumping rate and groundwater velocity in the fractures.

High velocities were previously avoided to prevent sloughing of biomass (Dupin and McCarty, 2000; Stewart and Fogler, 2001), but have also been connected to the development of more homogenous and compact distribution of biomass from redeposition (Okubo and Matsumoto, 1979; Taylor and Jaffe, 1990). The lack of oscillations in the transmissivity measurements during the field trial suggests that sloughing didn't occur on a scale detrimental to the development of the biobarrier. The distribution of bioclogging may also be attributable to the semi-passive operation of groundwater recirculation which promotes dispersive mixing between the injected solution and ambient groundwater that doesn't occur under a continuous injection withdrawal method (Devlin and Barker, 1996). Biological growth in the fracture connections between MTK204 and MTK201 is likely due to drift associated with the impact of natural hydraulic gradient.

PITs performed on a single borehole pair both prior to and during biostimulation yielded considerably different results based on the direction of source/observation borehole orientation. This is attributed to differences in fracture network geometry with each direction of flow (Lapcevic et al., 1999), changes with respect to natural flow gradient (Brutsaert, 1994) and variations in transmissivity of the source borehole.

Investigation of biobarrier longevity and the rate and magnitude of transmissivity recovery has varied in previous lab studies (Kim and Fogler, 2000; Ross et al., 2007; Seifert and Engesgaard, 2007). A rebound, or increase in transmissivity began to occur across the bioclogged area within 14 days following biostimulation, but clogging also continued to reduce transmissivity by more than two orders of magnitude after more than a month of starvation in the regions of most extensive growth. Rebound rates are thought to be a result of the microorganisms ability to form recalcitrant biomass and to degrade EPS for consumption (Thullner, 2010). Transmissivity rebound in the fracture connections of the project boreholes occurred at the highest rate in regions

where bioclogging had caused decreased transmissivity most extensively. This may be due to both the lack of nutrients under the more stagnant groundwater flow conditions and limited ability for the biofilm to degrade its own biomass for consumption as a carbon source. The poor biobarrier persistence of this study may also be correlated to the low C:N ratio (10) of the injected substrate. Investigation of C:N ratios from 6 to 80 by Avenimelech and Nevo (1964) found lower ratios lead to fast biological growth, with less EPS that display poor persistence during starvation. They also found that higher ratios led to slower growth rates with more EPS production and increased persistence.

2.6.2 Tracer Experiments

In laboratory studies conducted previously in single fractures, bioclogging has been shown to influence solute advection, dispersion, diffusion and adsorption (Hill and Sleep, 2002; Sharp et al, 1999; Charbonneau et al, 2006). Typically in closed systems (eg. sand columns or discrete lab factures), bioclogging-induced reductions in transmissivity lead to increases in flow velocity and dispersion. As the rates of groundwater flow are increased, the effects of diffusion and adsorption are diminished (Arnon et al., 2005). In this biostimulation field trial where the flow system is open, bioclogging is resulted in the development of more tortuous flow pathways, increasing dispersion but not velocity. This is illustrated in the post-biostimulation BTC measured in the observation borehole (Figure 7) which had later initial and peak arrival times, a more dispersed leading edge and a diminished peak magnitude relative to the pre-stimulation experiment. Thus the results of the clogged system tracer experiment are thought to represent biobarrier formation in the preferential flow pathways between the recirculating borehole pair with extended lateral distribution in the direction of natural groundwater hydraulic gradient. With significant reductions in transmissivity in the preferred pathways (as described above), tracer transport experiences a

more dispersed, tortuous route similar to results reported in Ross et al., (2007). This spreading effect and increased transverse dispersion consequently led to increased mass of tracer transported out of the capture zone of the withdrawal borehole thus accounting for the decreases in mass recovery observed in Figure 7. Alternatively, the biomass itself may have captured some of the tracer. Further laboratory studies are required to resolve this.

2.6.3 Thermal Stimulation

Consistent values throughout each borehole temperature monitoring location during the field trial would indicate a vertical flow regime in the injection borehole (Figure 8), and minimal loss or gain of fluid along the 10 m to 20 m depth section of both injection and withdrawal boreholes (Figure 9). The observed increase in temperature at 10 m BTOC in MTK203 is likely caused by the hydraulic connection to the injection borehole. This connection appears to be more isolated between the recirculating borehole pair than the fractured intervals at greater depths. This is determined by observing the temperature spikes in MTK202 compared to their arrival at the shallow levelogger in MTK203. The same temperature spikes are not evident at the deeper levelogger, which instead displays a more mixed, but larger thermal breakthrough. These temperature breakthroughs corroborate the estimated transmissivities of each fracture zone. The temperature rise at the withdrawal borehole is attributed to horizontal heat transport in discrete fractures and the dissipation of heat from the tubing returning pumped groundwater to the aboveground recirculation system.

The shape of daily temperature rise curves in MTK203 exhibit conventional transport breakthrough in an injection withdrawal flow field. Some changes in the peak can be observed over the biostimulation period as flattening of the peak occurs with increased bioclogging at the

10 mbgs location. This suggests microbial growth is most prevalent in the preferential groundwater flow pathways, forcing spreading and a more tortuous transport route of the warm fluid. The arrival peaks at both locations in the withdrawal borehole diminish as bioclogging increases during biostimulation. This also supports the results of the tracer experiment suggesting that clogging in dominant flow pathways has caused the spreading and increased transverse dispersion of heat during transport leading to loss outside the capture zone of the pumping borehole. The absorption of heat and lissamine into the biomass may also account for some mass tracer loss. The temperature measurements suggest that no lasting heating of the host rock occurred over the biostimulation phase.

2.6.4 Chemical Stimulation and the impact on the Groundwater Geochemistry

Although analytical results for ORP and DO in recirculating groundwater showed evidence of increasing biological activity, most other geochemical parameters of interest showed no significant fluctuations throughout the field trial (see Appendix H and Appendix I for more detailed results). This lack of observed geochemical impacts in major ionic species illustrates both the difficulties associated with open borehole sampling and the risk in relying on geochemical evidence alone to determine the presence of bacterial growth.

Changes in groundwater geochemistry may also be used to evaluate factors other than biological activity that can contribute to reductions in subsurface transmissivity. Mineral precipitation and entrapped poorly soluble gases generated by denitrifying bacteria or methanogens are mechanisms with potential for clogging of voids in geologic media (Baveye et al., 1998). Precipitations of ferrous hydroxides and $CaCO_3$ minerals have been observed in limestone environments, resulting in increasing values of groundwater pH (Ross et al., 2001). The slight

decreasing trend in pH we observed, suggests the contribution of mineral precipitation to reductions in transmissivity was negligible in this study. Although no increases in dissolved nitrogen or methane were measured during biostimulation, dilution from wellbore storage effects may have diminished changes in groundwater geochemistry. Aerobic conditions were maintained in recirculating groundwater throughout biostimulation, but in severely clogged regions no longer receiving sufficient delivery of an electron acceptor, anaerobic denitrifying or methanogenic reducing conditions may be present as seen in previous studies (Okubo and Matsumoto, 1983).

2.6.5 Biobarrier Formation

The hydraulic tests, tracer experiments and temperature results all suggest that biostimulation resulted in significant bioclogging which reduced the transmissivity of the discrete fracture network in the project boreholes. Geochemical and visual evidence confirms the increase in biological activity and suggests microbial growth is the principal source of the reductions in subsurface transmissivity. Although bioclogging was most extensive in preferential flow pathways between the injection and withdrawal boreholes, the effect of microbial growth is observed beyond the influence of the recirculation flow field. The spatial distribution of bioclogging is most significant downstream from the recirculation borehole pair under natural groundwater flow conditions. Rates of heat and solute transport were diminished due to spreading effects from bioclogged regions of the subsurface.

2.7 Conclusions

The objective of this study was to provide a preliminary investigation on the feasibility of applying bioclogging technology to a discrete fracture network at the field scale. The study investigated thermally and chemically enhanced biostimulation methods on an indigenous microbial community as a means to increase biological growth and clogging of the fractures. A field trial was conducted in a limestone and granite bedrock setting, including 14 days of biostimulation followed by 43 days under natural subsurface conditions. Bioclogging was evaluated using hydraulic tests, tracer experiments (fluorescent and heat) and geochemical monitoring of groundwater. From the results it can be concluded that:

1) the microorganisms indigenous to the project site can be biostimulated using thermal and chemical methods,
2) the microorganisms respond to biostimulation with increased biological growth, which can cause reductions in subsurface transmissivity and decrease the rate of solute mass transport in the impacted region,
3) Although bioclogging was most extensive in preferential flow pathways immediate to the injection borehole, operation of a semi-passive recirculation system induced the effects of biostimulation outside the influence of the injection borehole,
4) Evaluation of biobarrier development in a discrete fracture network should be completed using pulse interference tests and tracer experiments in addition to aqueous geochemistry in order provide an accurate assessment of the degree of clogging and the location where clogging occurred.
5) Fracture connections experiencing bioclogging exhibited rebounds in transmissivity within 14 days after the cessation of biostimulation, suggesting required maintenance may be necessary to maintain the integrity of the biobarrier.

These findings are significant as they demonstrate: (1) the feasibility of thermal and chemical biostimulation as a means to promote increased microbial activity under the project conditions; (2) that bioclogging can be achieved at the scale of a discrete fracture network in a field setting; and (3) the effectiveness of bioclogging used in biobarrier formation to reduce transmissivity and consequently decrease rates of solute transport in a fractured bedrock setting.

The results of this field trial have promising implications for the application of biobarriers as a groundwater containment technology in fractured rock aquifers. Further evaluation of the physical, biological and chemical factors influencing bioclogging are necessary before bioclogging can be considered a practical remedial option.

Chapter 3.0 Summary and Recommendations

Remedial approaches for fractured bedrock sites can be limited by both technical and financial challenges. Biostimulation induced bioclogging, used in the development of a biobarrier may provide a relatively low cost, low impact (no excavation) and low maintenance option for remedial design. Thermally and chemically enhanced biostimulation of indigenous microbial communities can increase subsurface biomass, biobarrier development and consequently lead to clogging in fractures and an overall reduction in transmissivity in a discrete fracture network. Microbial growth may also penetrate the matrix porosity of the bedrock further limiting contaminant transport and solidifying the microbial presence in the fracture.

Bioclogging in consolidated and unconsolidated media have been observed and examined in numerous laboratory studies. The physical, chemical and biological factors influencing growth have been well documented at the lab scale but extrapolation of these factors to the field scale has proved to be far from a trivial undertaking. Pilot-scale field applications have been completed in porous media and achieved promising results. No conclusive evidence of successful bioclogging field studies at the single fracture or discrete fracture network is known to have been published to date. In order to advance biobarrier technology towards industrial application in fractured rock, a better understanding of the controlling mechanisms of bioclogging and resultant effects on groundwater flow and transport need to be explored in a field setting.

In order to investigate the feasibility of biobarrier technology in fractured bedrock settings a field trial was conducted from September 2009 to April 2010. A review of existing literature, including close examination of prior studies within the research group was completed to improve understanding for the state of the practice and identify any knowledge gaps. The biostimulation field trial used thermal and chemical methods of biostimulation on indigenous microbial communities to increase biological activity and promote bioclogging. Thermal and chemical inputs were applied to groundwater recirculating between a selected borehole pair for 8 to 10 hours each day, then pumping was turned off and the local hydraulic gradient was returned to natural conditions. Hydraulic testing of the fracture connections in the boreholes estimated reductions in transmissivity up to five orders in magnitude due to the influence of bioclogging. Tracer experiment results showed significant reductions in the rate of solute mass transport in the affected region of the subsurface. Geochemical monitoring and visual observations determined the clogging to be related to increased biological growth. The bioclogged fracture connections began to exhibit rebounds in transmissivity within 14 days following biostimulation, but also

continued to reduce transmissivity in regions of the most extensive growth by more than two orders of magnitude after more than a month of starvation.

This study provides additional evidence of the potential for biobarrier technology as a remedial approach in fractured rock aquifers. It is recommended that future research in biobarrier technology performed at the field scale include a rigorous characterization of the site lithology, hydraulic parameters, fracture distribution, geochemical properties and microbial community. Incorporating pre-trial modeling of groundwater flow and transport properties for the affected area would prove useful in the design of the induced flow field and nutrient delivery methods.

Methods of biostimulation should be explored in microcosm experiments specific to each geological setting. Variations in thermal input and chemical type, concentration and delivery methods should be designed to maximize the magnitude and spatial distribution of the response in biological activity. Physical, biological and chemical parameters governing the long term persistence of a developed biobarrier and the required maintenance to maintain a desired degree of clogging should be evaluated.

Future field trials should examine the ability of biobarrier technology to hydraulically contain or redirect a groundwater plume, simulating a practical industrial application.

References

Allison, D.G. (2003). The biofilm matrix. Biofouling 19 (2), 139–150.

Armstrong, D.K. and T.R. Carter (2006). An updated guide to the subsurface Paleozoic stratigraphy of southern Ontario; Ontario Geological Survey, Open File Report 6191, 214p.

Arnon, S, E. Aar, Z. Ronen, A. Yakirevich, and R. Nativ (2005). Impact of microbial activity on the hydraulic properties of fractured chalk. Journal of Contaminant Hydrology, 76, 315-336.

Avnimelech, Y., and Z. Nevo (1964). Biological clogging of sands. Soil Science, 98, 222–226.

Baveye, P., P. Vandevivere, B.L. Hoyle, P.C. DeLeo, and D.S. de Lozada (1998). Environmental impact and mechanisms of the biological clogging of saturated soils and aquifer materials. Critical Reviews Environmental Science Technology, 28 (2), 123–191.

Bayona, L. (2009). Effects of in-situ stimulation of natural biofilm on groundwater flow and back diffusion in a fractured rock aquifer, Queen's University, Kingston, Ontario.

Berkowitz, B. (2002). Characterizing flow and transport in fractured geological media: a review. Advances in Water Resources, 25, 861-884.

Bouchez, M., D. Blanchet, J.P. Vandecasteele (1995). Degradation of polycyclic aromatic hydrocarbons by pure strains and by defined strain associations: inhibition phenomena and cometabolism. Applied Environmental Microbiology, 43, 156-164.

Brutsaert, W. (1994). The unit response of groundwater outflow from a hillslope. Water Resources Research, 30:2759–2763

Butler, J.J., Jr., and E.J. Garnett (2000). Simple procedures for analysis of slug tests in formations of high hydraulic conductivity using spreadsheet and scientific graphics software, Kansas Geological Survey, Open File Report 2000-40.

Castegnier, F., N. Ross, R. Chapuis, L. Deschenes and R. Samson (2006). Long-term persistence of a nutrient-starved biofilm in a limestone fracture. Water Research, 40, 925-934.

Charbonneau, A., K.S. Novakowski, and N. Ross (2006). The effect of a biofilm on solute diffusion in fractured porous media. Journal of Contaminant Hydrology, 85(3-4), 212-228.

Cunningham, A.B., R.R. Sharp, R. Hiebert, and G. James (2003). Subsurface biofilm barriers for the containment and remediation of contaminated groundwater. Bioremediation Journal, 7(3), 151-164.

Cusack, F., S.Singh, C. McCarthy, J. Grieco, M. De Rocco, D. Nguyen, H. Lappin-Scott, and J.W. Costerton (1992). Enhanced oil recovery—Three-dimensional sandpack simulation

of ultramicrobacteria resuscitation in reservoir formation. Journal of General Microbiology, 138, 647-655.

Davey, M.E., D. Gevertz, W.A. Wood, J.B. Clark, and G.E. Jenneman (1998). Microbial selective plugging of sandstone through simulation of indigenous bacteria in a hypersaline oil reservoir. Geomicrobiology, 15, 335-352.

Dupin, H.J. and P.L.McCarty (2000). Impact of colony morphologies and disinfection on biological clogging in porous media. Environmental Science and Technology, 34 (8), 1513–1520.

Devlin, J. F., and J. F. Barker (1996). Field investigation of nutrient pulse mixing in an in situ biostimulation experiment. Water Resources Research, 32(9), 2869-2877.

Flemming, H.C., J. Wingender, C. Mayer, V. Korstgens and W.Borchard (2000). Cohesiveness in biofilm matrix polymers. In: Allison, D.G., Gilbert, P., Lappin-Scott, H.M., Wilson, M., (Eds.), Community Structure and Co-operation in Biofilms, 59th Symposium of the Society for General Microbiology. Cambridge University Press, Cambridge, pp. 87–105.

Flemming, H.C. and J. Wingender (2010). The biofilm matrix. Nature Reviews Microbiology, 8(9): 623-633.

Gleeson, T.P., (2009). Groundwater recharge, flow and discharge in a large crystalline watershed, Queen's University, Kingston, Ontario.

Hiebert, R., R. Sharp, A. Cunningham and G. James (2001). Development and demonstration of sub-surface biofilm barriers using starved bacterial cultures. Contaminated Soil, Sediment, and Water, 45-47.

Hill, D.D. and B.E. Sleep (2002). Effects of biofilm growth on flow and transport through a glass parallel plate fracture. Journal Contaminant Hydrology, 56(3), 227-246.

Kim, G. (2004). Hydraulic conductivity change of bio-barrier formed in the subsurface by the adverse conditions including freeze-thaw cycles. Cold Region Science and Technology, 38, 153-164.

Kim, D.S., and H.S. Fogler (2000). Biomass evolution in porous media and its effects on permeability under starvation conditions. Biotechnology Bioengineering. 69 (1), 47–56.

Knight, L.C. (2008). The effect of biostimulation on geochemical and microbiological conditions in an isolated dolostone fracture, Queen's University, Kingston, Ontario.

Lapcevic, P.A., K.S. Novakowski, E.A. Sudicky (1999). Groundwater Flow and Solute Transport in Fractured Media. Chapter 17, The Handbook of Groundwater Engineering. CRC Press LLC.

Lappin-Scott, H.M., F. Cusack, and J.W. Costerton (1988). Nutrient resuscitation and growth of starved cells in sandstone cores: A novel approach to enhance oil recovery. Applied and Environmental Microbiology, 54, 1373-1382.

Leys, N.M., L. Bastiaens, W. Verstraete, and D. Springael (2005). Influence of the carbon/nitrogen/phosphorus ratio on polycyclic aromatic hydrocarbon degradation by Mycobacterium and Sphingomonas in soil. Applied Microbiology Technology, 66(6), 726-736.

M. S. Thompson &Associates Ltd. (1998). Phase I & II Environmental Site Assessment, Ministry of Transportation Regional Complex, Kingston, Ontario.

M. S. Thompson &Associates Ltd. (1999). Phase II & III Environmental Site Assessment, Ministry of Transportation Regional Complex, Kingston, Ontario.

Milloy, C.A. (2007). Measurement of hydraulic head for the evaluation of groundwater recharge to discrete fracture zones in a crystalline bedrock aquifer, Queen's University, Kingston, Ontario.

Miralles-Wilhelm, F., L.W. Gelhar (1996). Stochastic analysis of transport and decay of a solute in heterogeneous aquifers. Water Resources Research. 32 (12), 3451–3459.

Mutch, R.D., J.I. Scott, and D.J. Wilson (1993). Clean-up of fractured rock aquifers: Implications of matrix diffusion. Environmental Monitoring and Assessment, 24, 45-70.

Novakowski, K.S. (1988). Comparison of fracture aperture widths determined from hydraulic measurements and tracer experiments, Proc. 4th Can./Am. Conf. Hydrol. Banff, Alberta, pp. 68–80.

Novakowski, K.S. (1989). Analysis of pulse interference tests. Water Resources Research, 25(11): 2377-2387.

Novakowski, K.S., P. Lapcevic, G. Bickerton, J. Voralek, L. Zanini, C. Talbot (2000). The development of a conceptual model for contaminant transport in the dolostone underlying Smithville, Ontario. Supporting Report for Step 5 of the Smithville Phase 4 Bedrock Remediation Program.

Okubo, T., and J. Matsumoto (1979). Effect of infiltration-rate on biological clogging and water-quality changes during artificial recharge. Water Resources Research 15 (6), 1536–1542.

Okubo, T., and J. Matsumoto (1983). Biological clogging of sand and changes of organic constituents during artificial recharge. Water Research, 17 (7), 813–821.

Ontario Geological Survey (2009). Aggregate Resources Inventory of Frontenac County, Southern Ontario; Ontario Geological Survey, Open File Report 6240, p.20-1 to 20-9.

Parker, B.L., R.W. Gillham, and J.A. Cherry (1994). Diffusive disappearance of immiscible-phase organic liquids in fractured geologic media, Ground Water, 32(5): 805-819.

Ross, N., R., Villemur, L. Deschenes, and R. Samson (2001). Clogging of a limestone fracture by stimulating groundwater microbes. Water Research, 35 (8), 2029–2037.

Ross, N. and G. Bickerton (2002). Application of biobarriers for groundwater containment at fractured bedrock sites. Remediation, Summer 2002, 5-21.

Ross, N., K.S. Novakowski, S. Lesage, L. Deschenes, and R. Samson (2007). Development and resistance of a biofilm in a planar fracture during biostimulation, starvation, and varying flow conditions. Journal of Environmental Engineering and Science, 6(4): 377-388.

Seifert, D., P. Engesgaard (2007). Use of tracer tests to investigate changes in flow and transport properties due to bioclogging of porous media. Journal of Contaminant Hydrology. 93, 57–71.

Sharp, R.R., R. Gerlach, and A. Cunningham (1999). Bacterial transport issues related to subsurface biobarriers. In A. Leeson & B.C. Alleman (Eds.), In situ and on-site bioremediation proceedings of the Fifth International In Situ and On-Site Bioremediation Symposium, San Diego, California. Columbus, OH: Battelle Press.

Shaw, J.C., B. Bramhill, N.C. Wardlaw, and J.W. Costerton (1985). Bacterial fouling in a model core system. Applied Environmental Microbiology, 49(3), 693-701.

SNC Lavalin Engineers & Constructors Inc. (2002). Groundwater Samping and Subsurface Investigation, 355 Counter Street, Kingston Ontario. Final Report to Ontario Reality Corporation.

Schauerte (2011). *Graduate research in progress.*

Stewart, T.L. and H.S. Fogler (2001). Biomass plug development and propagation in porous media. Biotechnology and Bioengineering, 72 (3), 353–363.

Steimle, R. (2002). The state of the practice: characterizing and remediating contaminated groundwater at fractured rock sites. Remediation, Summer 2002, 23-33.

Taylor, S.W. and P.R. Jaffe (1990). Biofilm growth and the related changes in the physical properties of a porous-medium. 1. Experimental investigation. Water Resources Research 26 (9), 2153–2159.

Thullner, M. (2010). Comparison of bioclogging effects in saturated porous media within one- and two-dimensional flow systems. Ecological Engineering. 36, 176–196

Van der Kamp, G. (1976). Determining aquifer transmissivity by means of well response tests: The underdamped case. Water Resources Research 12, no. 1:71–77.

Vandevivere, P. and P. Baveye, (1992). Effect of bacterial extracellular polymers on the saturated hydraulic conductivity of sand columns. Applied Environmental Microbiology, 58(5), 1690-1698.

Zlotnik, V.A. and V.L. McGuire (1998). Multi-level slug tests in highly permeable formations. 1. Modification of the Springer-Gelhar (SG) model. Journal of Hydrology, 204:271-282.

Appendices

In addition to the following appendices, the attached disk contains analytical calculations performed for slug test and pulse interference test interpretation.

Appendix A –Tracer Experiment Results

Table A1. Experimental setup, conditions and results of tracer experiments.

Experimental Conditions						**Tracer Injection**			**Tracer Breakthrough**		
Date	***Test Type***	***Injection Borehole***	***Withdrawal Borehole***	***Depth of Pump (m)***	***Flow Rate (Lpm)***	***Mass (g)***	***Volume (L)***	***Concentration (mg/L)***	***Time to Peak Arrival (min)***	***Peak (mg/L)***	***Injection Concentration/ Breakthrough Peak Concentration (%)***
21-Jul-09	Natural Gradient	203	NA	NA	NA	75	200	375	50 (201)	0.52 (201)	0.139
									400 (203)	0.14 (203)	0.037
6-Aug-09	Dipole	202	203	20	4	20	10	2000	120	3.6	0.180
12-Aug-09	Dipole	200	203	20	4	20	10	2000	40	1.9	0.095
6-Nov-09	Dipole	203	201	23	4	1.01	5	202	117	0.11	0.054
8-Nov-09	Dipole	203	201	23	5	3.04	21	145	37	0.16	0.111
20-Nov-09	Dipole	204	203	20	5	5.832	12	486	180	0.105	0.022
23-Nov-09	Dipole	204	203	20	5	5.01	20	251	72	0.3	0.120
13-Dec-10	Dipole	202	203	20	5	10.26	21	489	160	1.3	0.266
26-Jan-10	Dipole	202	203	23	15	10.377	330	31	25	5.3	16.855
27-Jan-10	Dipole	202	203	23	10	9.752	357	27	60	2.8	10.250
28-Jan-10	Dipole	202	203	23	10	10.363	365	28	60	2.6	9.158
11-Mar-10	Dipole	202	203	23	15	10.59	330	32	33	3.6	11.218

Note: Tracer experiments perform prior to December 13, 2010 used a FLUTe injection system in the injection borehole.

Extrapolation of lissamine concentration beyond the measured data was completed using power law trendlines generated in Microsoft Excel. Lissamine concentration values from the concentration peak to end of available measured data were used to generate each trendline.

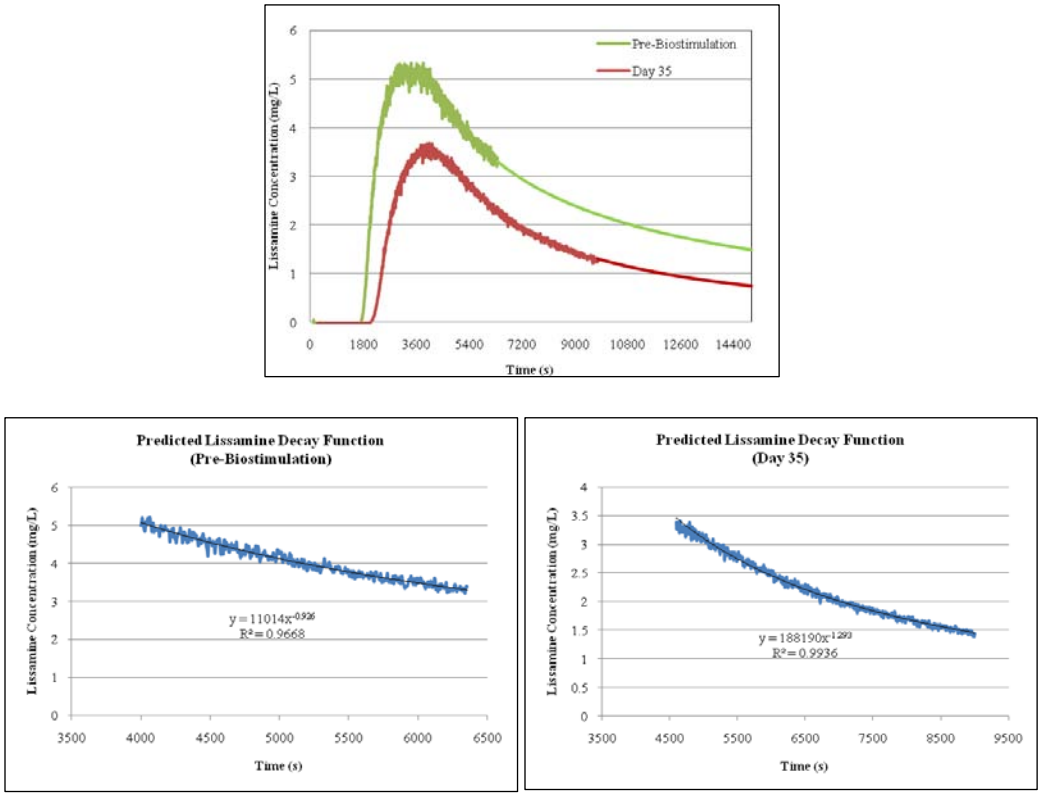

Figure A1. Trendline equations and regression used in the extrapolation of lissamine concentration values.

Appendix B – Aboveground Recirculation System

Table A2. Dimensions of recirculation system components.

Component	Internal Diameter (mm)	Length (m)	Volume (L)
MTK203 Wellbore	96	21	152.0
Extraction Tubing	19	32.1	9.1
Heated Reservoir (0.45 m depth)	-	-	365
Insulated Coil	25.4	35	18.1
Injection Tubing	19	16.5	4.7
MTK202 Wellbore	96	21	152.0
Total Volume*			***701***

*Doesn't include volume of fracture connections

Appendix C – Fluorometer Calibration

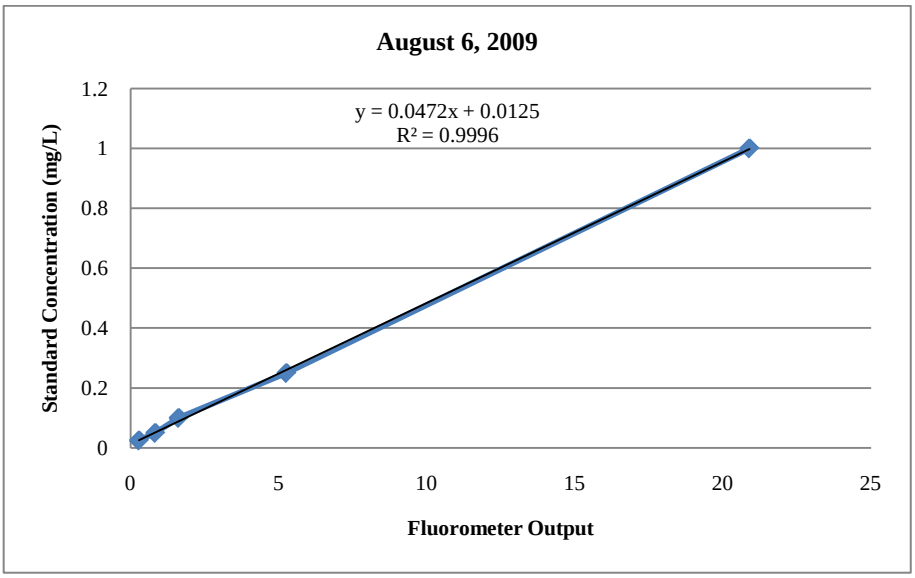

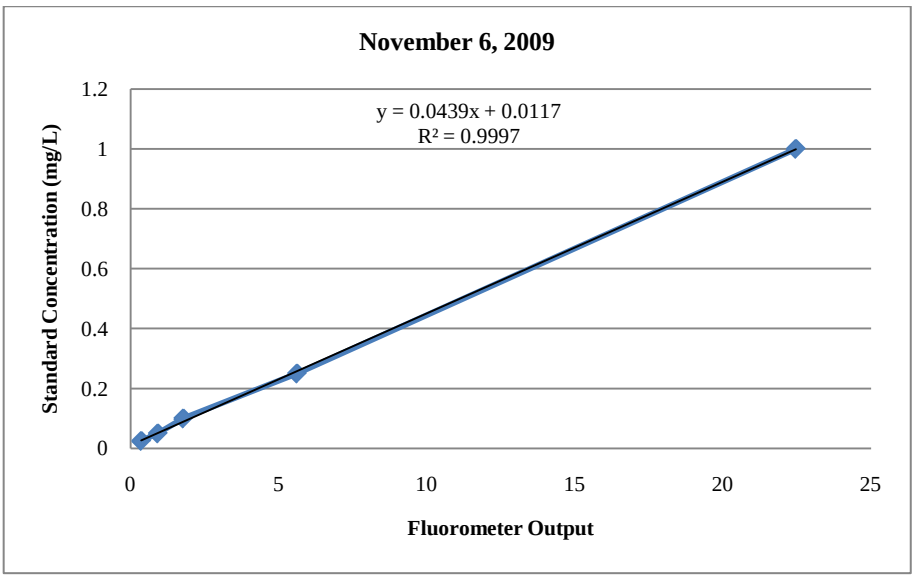

Appendix C – Fluorometer Calibration *continued*

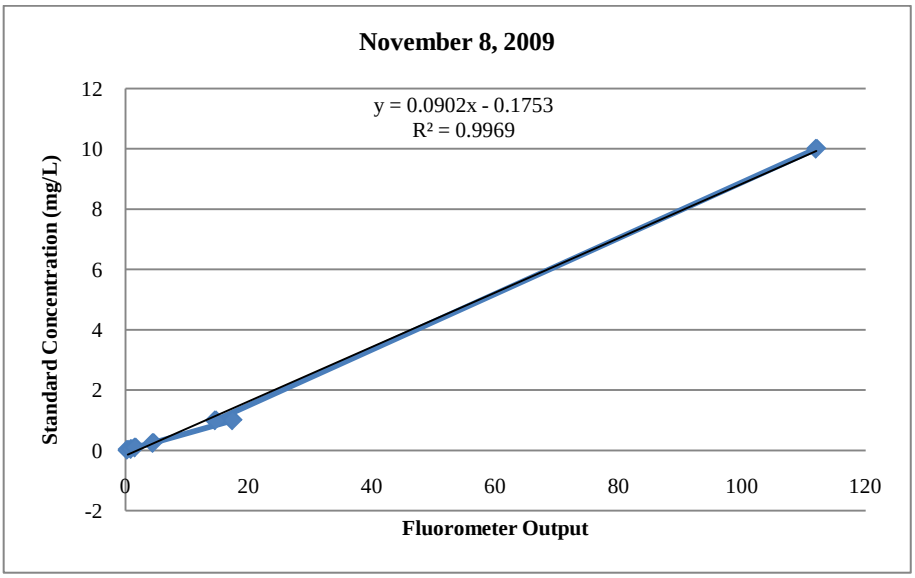

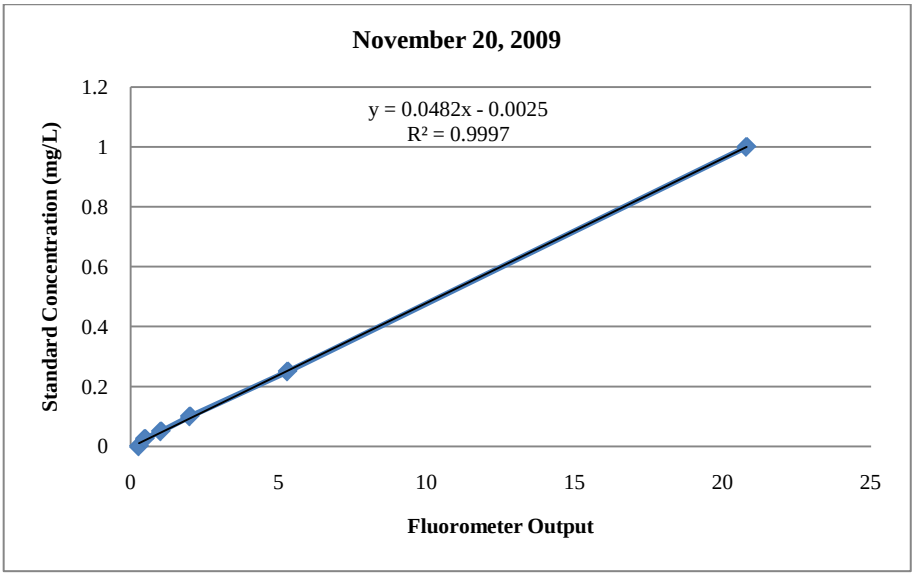

Appendix C – Fluorometer Calibration *continued*

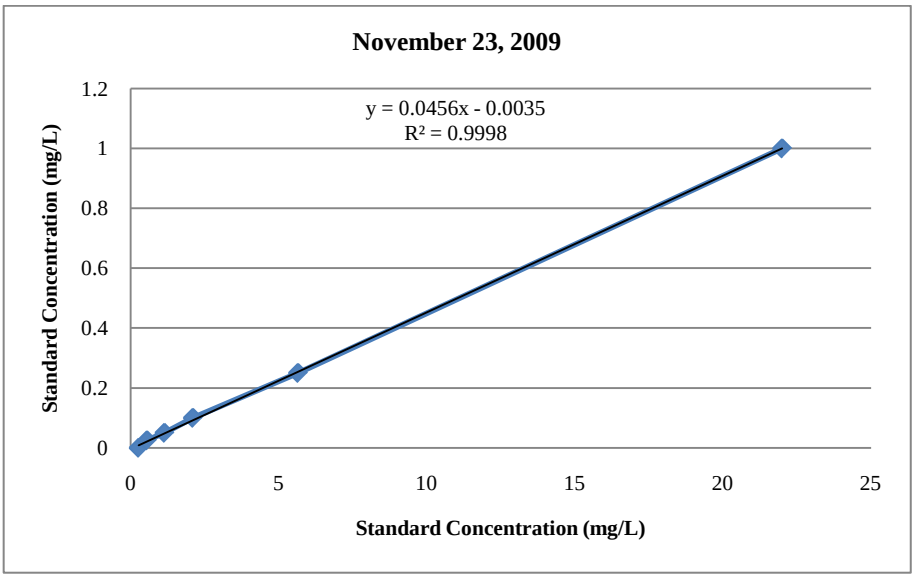

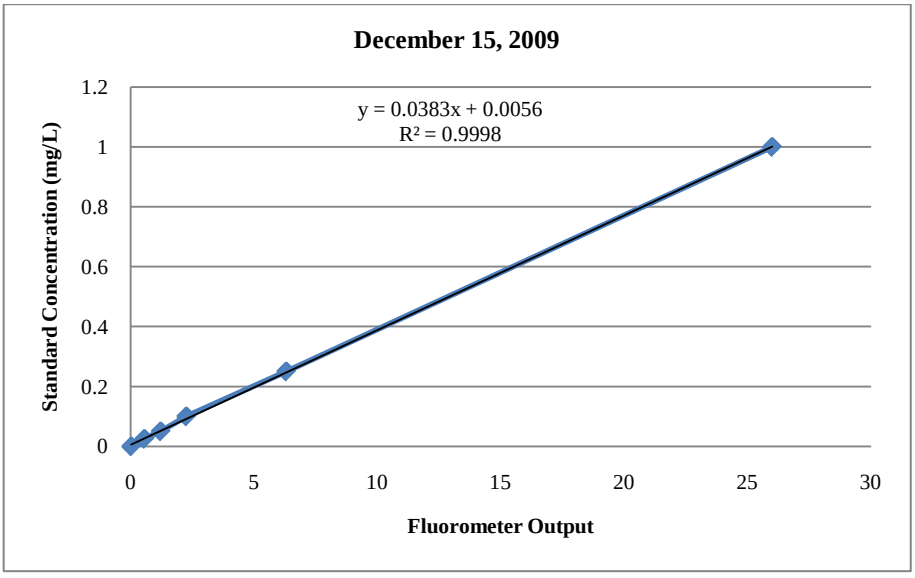

Appendix C – Fluorometer Calibration *continued*

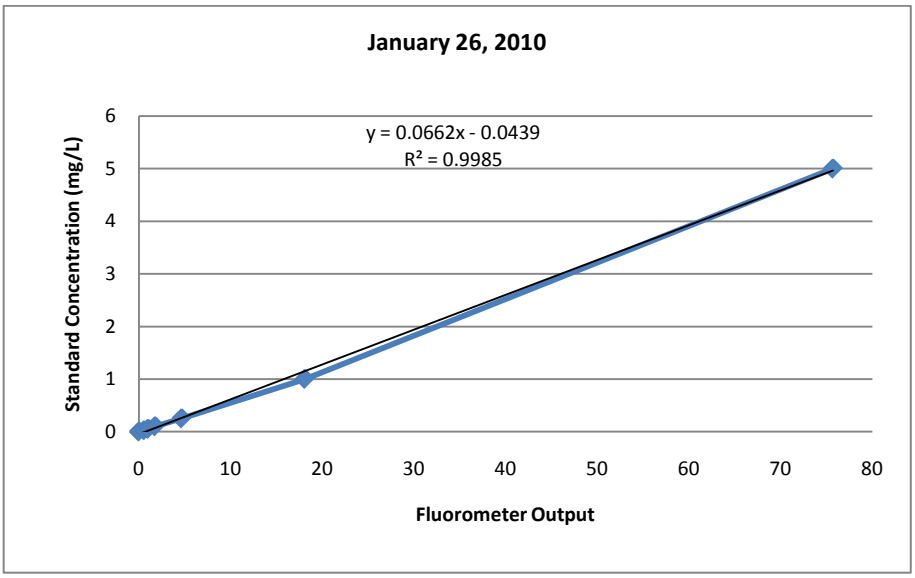

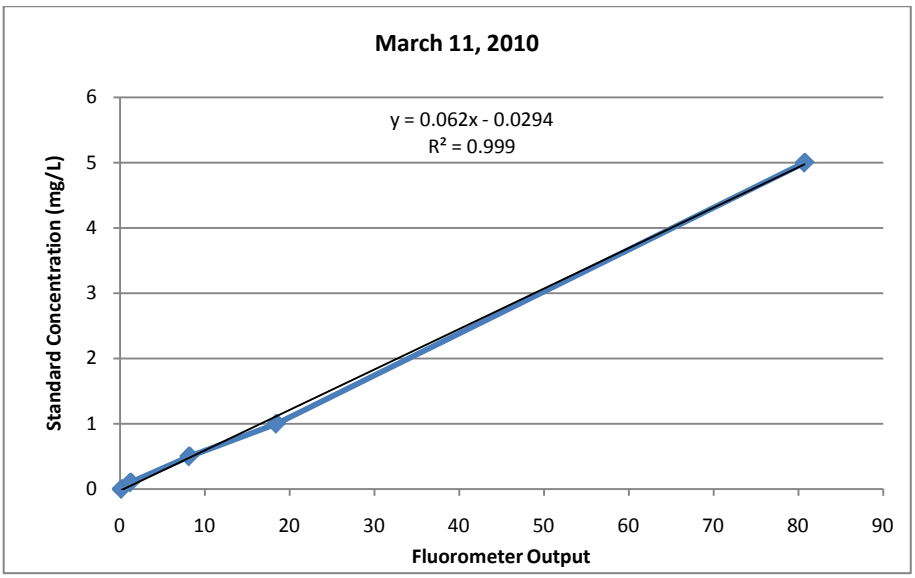

Appendix D – Nutrient Injection Calculations

Table A3. Composition of nutrient injections.

Source	Nutrient Concentration (g/mL)		
	Carbon	**Nitrogen**	**Phosphorus**
Sodium Lactate (60% w/w)	0.25	0.00	0.00
Miracle Gro (4:12:4)*	0.00	0.05	0.06
LiquaFeed (12:4:8)*	0.00	0.14	0.02

Source	Injection Volumes (L)	
	A	**B**
Sodium Lactate (60% w/w)	3.714	4.000
Miracle Gro (4:12:4)*	0.186	0.150
LiquaFeed (12:4:8)*	0.743	0.805

	Carbon	**Nitrogen**	**Phosphorus**
Mass per Injection A (g)	931.49	100.76	14.67
C-N-P Ratio	100	11	2
Mass per Injection B (g)	1003.22	109.17	15.89
C-N-P Ratio	100	11	2

*Ratios given with commercial fertilizers represent a C:N:P mass ratio.

Appendix E – Nutrient Injection Events

Table A4. Nutrient injection events

Day	Recirculation started	Injection Time	Recirculation stopped	Sodium Lactate (L)	Miracle Gro (L)	Liquafeed (L)
05-Feb-10	11:35	12:36	20:47	3.714	0.186	0.743
06-Feb-10	9:36	12:07	19:13	3.714	0.186	0.743
07-Feb-10	9:20	10:59	18:30	3.714	0.186	0.743
08-Feb-10	9:15	11:50	21:30	3.714	0.186	0.743
09-Feb-10	11:00	12:10	19:11	3.714	0.186	0.743
10-Feb-10	8:40	10:13	18:56	3.714	0.186	0.743
11-Feb-10	9:30	11:15	19:23	3.714	0.186	0.743
12-Feb-10	9:50	12:45	20:09	3.714	0.186	0.743
13-Feb-10	10:14	11:24	21:40	3.714	0.186	0.743
14-Feb-10	10:23	11:27	18:32	4.000	0.150	0.805
15-Feb-10	9:00	11:08	18:30	4.000	0.150	0.805
16-Feb-10	9:30	10:45	20:05	4.000	0.150	0.805
17-Feb-10	8:55	10:20	18:28	4.000	0.150	0.805
18-Feb-10	10:15	11:45	19:37	4.000	0.150	0.805

Appendix F– Slug Test Results

Table A5. Slug test results in boreholes MTK200 and MTK201.

Borehole		MTK200				MTK201			
Parameter		T (m^2/s)	H_o	Response	Reduction in T (%)	T (m^2/s)	H_o	Response	Reduction in T (%)
Pre-Trial	**18-Aug-09**	7.0×10^{-4}	1.9	O	NA	*NTP*			
	1-Nov-09	9.3×10^{-4}	0.50	O	NA	2.7×10^{-3}	0.466	C	NA
	30-Jan-10	*NTP*				*NTP*			
	Average	8.11×10^{-4}				2.67×10^{-3}			
Day 5		*NTP*				*NTP*			
Day 9									
Day 11									
Day 12									
Day 14									
Day 18		9.0×10^{-4}	0.638	O	-10.7%	1.3×10^{-3}	0.406	C	50.0%
Day 29		8.7×10^{-4}	0.665	O	-6.8%	9.5×10^{-4}	0.391	C	64.3%
Day 57		8.1×10^{-4}	0.754	O	0.3%	1.2×10^{-3}	0.428	C	54.9%

NA: Not Applicable
NTP: No testing performed
Response: Overdamped (O), critically damped (C) and underdamped (U)

Table A6. Slug test results in boreholes MTK202 and MTK203.

Borehole		MTK202				MTK203			
Parameter		T (m^2/s)	H_o	Response	Reduction in T (%)	T (m^2/s)	H_o	Response	Reduction in T (%)
Pre-Trial	**18-Aug-09**	3.4×10^{-3}	0.974	U	NA	4.8×10^{-3}	1.071	U	NA
	1-Nov-09	2.9×10^{-3}	0.316	U	NA	6.7×10^{-3}	0.295	U	NA
	30-Jan-10	2.5×10^{-3}	0.359	U	NA	8.9×10^{-3}	0.262	U	NA
	Average	2.93×10^{-3}				6.8×10^{-3}			
Day 5		2.5×10^{-3}	0.295	C	14.5%	3.3×10^{-3}	0.245	C	51.0%
Day 9		1.5×10^{-3}	0.610	O	49.4%	2.5×10^{-3}	0.303	O	63.2%
Day 11		9.5×10^{-4}	0.809	O	67.7%	6.1×10^{-3}	0.305	U	10.9%
Day 12		7.4×10^{-4}	0.823	O	74.7%	4.4×10^{-3}	0.362	U	35.4%
Day 14		2.4×10^{-4}	0.937	O	91.7%	2.2×10^{-3}	0.316	C	67.1%
Day 18		2.9×10^{-4}	1.096	O	90.1%	1.9×10^{-3}	0.383	O	71.9%
Day 29		5.2×10^{-4}	0.761	O	82.1%	3.0×10^{-3}	0.458	C	56.4%
Day 57		1.5×10^{-3}	0.658	O	49.4%	2.6×10^{-3}	0.335	C	61.6%

NA: Not Applicable
NTP: No testing performed
Response: Overdamped (O), critically damped (C) and underdamped (U)

Table A7. Slug test results in boreholes MTK200 and MTK201.

Borehole		MTK204			
Parameter		T (m^2/s)	H_o	Response	Reduction in T (%)
Pre-Trial	**18-Aug-09**	7.6×10^{-3}	0.790	U	NA
	1-Nov-09	6.8×10^{-3}	0.228	U	NA
	30-Jan-10	*NTP*			
	Average	7.23×10^{-3}			
Day 5		*NTP*			
Day 9					
Day 11					
Day 12					
Day 14					
Day 18		4.4×10^{-3}	0.409	U	38.5%
Day 29		2.7×10^{-3}	0.382	U	63.1%
Day 57		3.6×10^{-3}	0.469	C	50.8%

NA: Not Applicable
NTP: No testing performed
Response: Overdamped (O), critically damped (C) and underdamped (U)

Appendix G – Pulse Interference Results

Table A8. Transmissivity (m^2/s) results from open borehole pulse interference tests (source borehole: MTK200 and MTK201)

Source Borehole		**MTK200**				**MTK201**			
Observation Borehole		**MTK201**	**MTK202**	**MTK203**	**MTK204**	**MTK200**	**MTK202**	**MTK203**	**MTK204**
Pre Trial	**18-Aug-09**	*NTP*	1.6×10^{-4}	9.2×10^{-5}	4.6×10^{-4}	*NTP*			
	1-Nov-09	9.2×10^{-4}	4.0×10^{-4}	9.2×10^{-4}	1.2×10^{-3}	5.8×10^{-2}	5.4×10^{-3}	6.9×10^{-1}	9.2×10^{-2}
	30-Jan-10	*NTP*				*NTP*			
	Average	9.2×10^{-4}	2.8×10^{-4}	5.1×10^{-4}	8.1×10^{-4}	5.8×10^{-2}	5.4×10^{-3}	6.9×10^{-1}	9.2×10^{-2}
Day 5		*NTP*				*NTP*			
Day 9									
Day 12									
Day 14									
Day 18		1.4×10^{-3}	3.4×10^{-5}	2.0×10^{-3}	7.7×10^{-4}	2.9×10^{-1}	1.2×10^{-4}	5.1×10^{0}	9.2×10^{-3}
Day 29		2.3×10^{-3}	5.1×10^{-5}	6.3×10^{-4}	6.6×10^{-4}	3.5×10^{-1}	3.6×10^{-4}	3.8×10^{0}	6.6×10^{-3}
Day 57		8.2×10^{-4}	3.1×10^{-4}	4.2×10^{-4}	5.1×10^{-4}	7.3×10^{-2}	1.0×10^{-3}	3.5×10^{0}	3.1×10^{-2}
Maximum Reduction %		11	88	17	37	0	98	0	93

NTP: No testing performed

Table A9. Transmissivity (m^2/s) results from open borehole pulse interference tests (source borehole: MTK202 and MTK203)

Source Borehole		**MTK202**				**MTK203**			
Observation Borehole		**MTK 200**	**MTK201**	**MTK203**	**MTK204**	**MTK200**	**MTK201**	**MTK202**	**MTK204**
Pre Trial	**18-Aug-09**	1.9×10^{-3}	*NTP*	3.5×10^{-2}	2.3×10^{-2}	1.2×10^{-2}	*NTP*	7.5×10^{-1}	2.9×10^{-2}
	1-Nov-09	1.0×10^{-3}	1.7×10^{-3}	4.0×10^{-1}	2.3×10^{-1}	7.9×10^{-3}	2.3×10^{-1}	2.3×10^{0}	1.7×10^{0}
	30-Jan-10	*NTP*		1.3×10^{-1}	*NTP*	*NTP*		5.4×10^{0}	*NTP*
	Average	1.5×10^{-3}	1.7×10^{-3}	1.9×10^{-1}	1.3×10^{-1}	9.7×10^{-3}	2.3×10^{-1}	2.8×10^{0}	8.8×10^{-1}
Day 5		*NTP*		2.5×10^{-3}	*NTP*	*NTP*		2.9×10^{0}	*NTP*
Day 9				1.2×10^{-3}				2.3×10^{-1}	
Day 12				9.2×10^{-5}				2.4×10^{-3}	
Day 14				1.9×10^{-5}				6.1×10^{-5}	
Day 18		1.9×10^{-5}	2.8×10^{-5}	9.2×10^{-6}	1.2×10^{-4}	2.1×10^{-3}	5.1×10^{0}	4.9×10^{-5}	5.8×10^{-3}
Day 29		3.3×10^{-5}	4.6×10^{-5}	7.1×10^{-5}	9.9×10^{-5}	3.7×10^{-2}	2.3×10^{-1}	1.2×10^{-3}	5.3×10^{-2}
Day 57		2.0×10^{-4}	4.3×10^{-4}	2.8×10^{-4}	7.7×10^{-4}	6.6×10^{-2}	5.8×10^{0}	1.2×10^{-2}	1.2×10^{-1}
Maximum Reduction %		99	98	10000	1000	78	0	10000	99

NTP: No testing performed

Table A10. Transmissivity (m^2/s) results from open borehole pulse interference tests (source borehole: MTK204)

Source Borehole		**MTK204**			
Observation Borehole		**MTK200**	**MTK201**	**MTK202**	**MTK203**
Pre Trial	**18-Aug-09**	5.8×10^{-3}	*NTP*	1.2×10^{0}	2.3×10^{1}
	1-Nov-09	4.6×10^{-3}	6.6×10^{-2}	4.6×10^{0}	5.8×10^{0}
	30-Jan-10	*NTP*			
	Average	5.2×10^{-3}	6.6×10^{-2}	2.9×10^{0}	1.4×10^{1}
Day 5		*NTP*			
Day 9					
Day 12					
Day 14					
Day 18		1.2×10^{-3}	4.2×10^{-3}	2.4×10^{-4}	3.3×10^{-1}
Day 29		1.5×10^{-3}	2.9×10^{-3}	7.7×10^{-4}	6.1×10^{-3}
Day 57		3.1×10^{-3}	6.6×10^{-3}	3.1×10^{-2}	1.0×10^{-2}
Maximum Reduction %		76	96	10000	1000

NTP: No testing performed

Table A11. Interval pulse interference test results

Test	Borehole	Orientation	Isolated Interval in Borehole (mBTOC)		$S = (\pi r_c^2)/(2\pi r_w^2 C_{DS})$	$T = t_D(r_w^2 S)/t_L$
			Top	***Bottom***	**(dim)**	**(m^2/s)**
15-Jan-10						
1	202	Source	25.89	28.49	1.0×10^{-6}	1.4×10^{-6}
	203	Observation	24	26.6		
2	202	Source	25.89	28.49		7.7×10^{-6}
	203	Observation	28.46	Bottom		
3	202	Source	28.45	Bottom		2.5×10^{-5}
	203	Observation	28.46	Bottom		
4	202	Source	28.45	Bottom		1.2×10^{-6}
	203	Observation	24	26.6		
5-Mar-10						
1	202	Source	25.89	28.49	1.0×10^{-6}	1.4×10^{-6}
	203	Observation	24	26.6		
2	202	Source	25.89	28.49		4.4×10^{-7}
	203	Observation	28.46	Bottom		
3	202	Source	28.45	Bottom		1.0×10^{-7}
	203	Observation	28.46	Bottom		
4	202	Source	28.45	Bottom		1.1×10^{-6}
	203	Observation	24	26.6		

Appendix H – Groundwater Sampling Chemistry and Microbiology Results

Table A12. Analytical results of bacteriological parameters in groundwater samples collected during the field trial.

Date	**Sample No**	**Bacteriological**		
Parameter		**Heterotrophic Plate Count**	**Pseudo. a.**	**Iron Bacteria**
units		cfu/ML	cfu/100ml	cts/1mL
detection limit		10	1	10
26-Oct-09	1026-1	>2000	0	35150
8-Feb-10	0208-1	>2000	0	138000
13-Feb-10	0213-1	>2000	>200	69560
23-Feb-10	0223-1	173000	<2	35150

Table A13. Analytical results of redox parameters in groundwater samples collected during the field trial.

Date	**Sample No**	**Redox Conditions**							
Parameter		**Methane**	**Sulphate**	**Hydrogen Sulphide**	**Iron**	**Nitrite**	**Nitrate**	**Ammonia + Ammonium**	**Manganese**
units		**L/m3**	**mg/L**	**mg/L**	**mg/L**	**mg/L**	**mg/L**	**mg/L**	**mg/L**
detection limit		**0.01**	**1**	**0.01**	**0.005**	**0.1**	**0.1**	**0.05**	**0.001**
2-Nov-09	1102-1		55	<0.01	0.011	< 0.1	0.3	0.09	0.001
8-Feb-10	0208-1	<0.01	54	< 0.01	0.005	0.2	0.4	<0.05	0.004
13-Feb-10	0213-1	<0.01	50	<0.01	0.022	< 0.1	< 0.1	0.05	0.009
23-Feb-10	0223-1	0.01	58	<0.01	0.022	<0.1	0.5	<0.05	0.003

Table A14. Analytical results of general chemistry parameters in groundwater samples collected during the field trial.

Date	**Sample No**	**General Chemistry**							
Parameter		**Alkalinity (as CaCO3)**	**pH**	**Conductivity**	**Colour**	**Turbidity**	**Fluoride**	**Chloride**	**o-Phosphate (P)**
units		**mg/L**		**umho/cm**	**TCU**	**NTU**	**mg/L**	**mg/L**	**mg/L**
detection limit		**3**		**1**	**2**	**0.2**	**0.1**	**1**	**0.01**
2-Nov-09	1102-1	322	7.7	1010	< 2	0.3	0.7	106	0.06
8-Feb-10	0208-1	378	8.12	1050	< 2	0.9	0.6	84	0.03
13-Feb-10	0213-1	385	7.81	992	< 2	3.2	0.6	76	0.05
23-Feb-10	0223-1	356	7.71	1010	<2	0.4	0.6	96	0.04

Table A15. Analytical results of general chemistry parameters in groundwater samples collected during the field trial.

Date	**Sample No**	**General Chemistry**						
Parameter		**Hardness (as CaCO3)**	**Calcium**	**Copper**	**Magnesium**	**Potassium**	**Sodium**	**Zinc**
units		**mg/L**	**mg/L**	**mg/L**	**mg/L**	**mg/L**	**mg/L**	**mg/L**
detection limit		**1**	**0.02**	**0.002**	**0.01**	**0.1**	**0.2**	**0.005**
2-Nov-09	1102-1	394	72.9	0.002	51.5	5.1	64.5	0.018
8-Feb-10	0208-1	377	72.8	0.002	47.5	4.3	54.3	0.021
13-Feb-10	0213-1	390	72.9	< 0.002	50.5	5	65.1	0.031
23-Feb-10	0223-1	394	74.5	<0.002	50.5	4.5	61	<0.005

Appendix I – Geochemical Monitoring of Recirculating Groundwater

Table A16. YSI monitoring results of water quality parameters in recirculating groundwater during biostimulation.

Day	Time	Temperature (°C)	Conductivity (µS/cm)	Conductivity (µS/cm)	Total Dissolved Solids (g/L)	Salinity	Reading Location
4-Feb-10	14:35:00	9.85	954	678	0.622	0.48	Withdrawal Well (203)
4-Feb-10	15:15:00	9.85	957	680	0.619	0.47	Withdrawal Well (203)
5-Feb-10	12:30:00	10.6	949	688	0.617	0.47	Withdrawal Well (203)
5-Feb-10	14:42:00	10.56	1378	998	0.9	0.69	Withdrawal Well (203)
6-Feb-10	11:58:00	10.12	994	711	0.645	0.49	Withdrawal Well (203)
6-Feb-10	14:53:00	10.2	1007	714	0.654	0.5	Withdrawal Well (203)
7-Feb-10	10:51:00	8.22	994	675	0.65	0.49	Withdrawal Well (203)
8-Feb-10	11:15:00	8.29	991	680	0.645	0.49	Withdrawal Well (203)
8-Feb-10	16:00:00	10.01	1138	812	0.74	0.57	Withdrawal Well (203)
9-Feb-10	12:25:00	9.85	985	700	0.641	0.44	Withdrawal Well (203)
10-Feb-10	09:42:00	8.2	940	637	0.61	0.46	Withdrawal Well (203)
10-Feb-10	19:07:00	8.83	1051	726	0.683	0.52	Withdrawal Well (203)
11-Feb-10	11:50:00	18.91	1010	896	0.657	0.5	Withdrawal Well (203)
11-Feb-10	12:20:00	10.54	994	719	0.647	0.49	Withdrawal Well (203)
11-Feb-10	16:10:00	9.6	1147	810	0.745	0.57	Withdrawal Well (203)
11-Feb-10	19:20:00	8.9	1062	734	0.69	0.53	Withdrawal Well (203)
12-Feb-10	10:10:00	6.99	1022	670	0.664	0.51	Withdrawal Well (203)
12-Feb-10	12:10:00	8.56	1015	696	0.68	0.5	Withdrawal Well (203)
12-Feb-10	13:30:00	10.31	1663	1196	1.081	0.85	Withdrawal Well (203)
12-Feb-10	20:10:00	8.89	1078	746	0.7	0.54	Withdrawal Well (203)

Day	Time	Temperature (°C)	Conductivity (µS/cm)	Conductivity (µS/cm)	Total Dissolved Solids (g/L)	Salinity	Reading Location
13-Feb-10	10:32:00	8.33	1011	689	0.657	0.5	Withdrawal Well (203)
13-Feb-10	21:40:00	7.82	1064	715	0.692	0.53	Withdrawal Well (203)
14-Feb-10	10:40:00	7.2	1033	681	0.671	0.51	Withdrawal Well (203)
14-Feb-10	14:49:00	9.85	1179	838	0.766	0.59	Withdrawal Well (203)
14-Feb-10	18:30:00	9.62	1087	768	0.706	0.54	Withdrawal Well (203)
15-Feb-10	09:25:00	28.1	3.23	4.52	125.6	-55.8	Withdrawal Well (203)
15-Feb-10	17:30:00	9.25	1102	766	0.713	0.55	Withdrawal Well (203)
16-Feb-10	09:45:00	8.63	1017	699	0.661	0.51	Withdrawal Well (203)
16-Feb-10	10:40:00	9.65	1017	727	0.661	0.51	Withdrawal Well (203)
16-Feb-10	12:56:00	9.48	1269	913	0.825	0.64	Withdrawal Well (203)
16-Feb-10	19:58:00	8.84	1079	744	0.701	0.54	Withdrawal Well (203)
17-Feb-10	09:05:00	8.26	1017	693	0.661	0.51	Withdrawal Well (203)
18-Feb-10	14:30:00	10.42	995	718	0.647	0.49	Withdrawal Well (203)
18-Feb-10	15:30:00	10.42	1013	732	0.659	0.5	Withdrawal Well (203)
5-Feb-10	12:36:00	19.1	4720	4240	3.07	2.5	Reservoir (Post Injection)
5-Feb-10	14:42:00	18.2	1502	1310	0.98	0.76	Reservoir (Post Injection)
6-Feb-10	12:16:00	23.9	4524	4430	2.945	2.41	Reservoir (Post Injection)
8-Feb-10	12:00:00	14.93	4690	3787	3.049	2.52	Reservoir (Post Injection)
8-Feb-10	21:00:00	14.69	1070	859	0.696	0.53	Reservoir (Post Injection)
9-Feb-10	17:40:00	15.9	1145	945	0.744	0.57	Reservoir (Post Injection)

Appendix J – Images of Field Work

Figure A2. Image of insulated aboveground reservoir containing immersion heater and mixer.

Figure A3. Image of insulated aboveground reservoir and 25.4 mm ID polyethylene tubing in coil.

Figure A4. Image of biological growth in recirculated groundwater left stagnant in aboveground reservoir over night.

Figure A5. Image of solid lissamine fluorescent dye mixing in reservoir during tracer experiment.

Figure A6. Image of 13 mm ID tubing gravity draining the aboveground reservoir into the injection borehole (MTK202).

Figure A7. Image of nutrient solution preparation.

Figure A8. Image of tent enclosing workspace and components of the recirculation system.

Figure A9. Image of packer assembly for interval pulse interference testing.